*eng*

*Review*

# Direct Air Capture (DAC) for Achieving Net-Zero $CO_2$ Emissions: Advances, Applications, and Challenges

**Guihe Li** [1,2] **and Jia Yao** [1,3,*]

[1] College of Engineering and Physical Sciences, University of Wyoming, Laramie, WY 82071, USA; guiheli@alumni.upenn.edu
[2] School of Engineering and Applied Science, University of Pennsylvania, Philadelphia, PA 19104, USA
[3] Biodesign Institute, Arizona State University, Tempe, AZ 85287, USA
* Correspondence: jyao46@asu.edu

**Abstract:** Carbon dioxide ($CO_2$), as the primary greenhouse gas, has significant impacts on global climate change, leading to severe and irreversible adverse consequences for ecosystems and human environments. To address the issue of excessive $CO_2$ emissions, efforts in recent years have yielded significant progress in the development of clean energy sources and the promotion of carbon capture, utilization, and storage (CCUS) technologies. Conventional $CO_2$ capture techniques are limited in addressing global atmospheric $CO_2$ excess effectively, as they target only high-concentration $CO_2$ emissions and require implementation at specific emission points. Direct air capture (DAC) technology has emerged as a promising solution due to its flexibility in deployment, avoidance of land competition, and ability to capture legacy $CO_2$ emissions. Additionally, DAC offers opportunities for producing synthetic clean fuels, thereby reducing reliance on traditional fossil fuels and aiding in reducing greenhouse gas emissions. This study provides a comprehensive review of DAC technology, encompassing its principles, technological advancements, real-world applications, challenges, and future research directions. By offering insights into the current state and potential of DAC technology, this study aims to guide global efforts in scaling up DAC deployment, ultimately contributing to achieving global carbon neutrality or even negative emissions.

**Keywords:** direct air capture (DAC); carbon neutrality; net-zero $CO_2$ emissions; liquid DAC (L-DAC); solid DAC (S-DAC); electro-swing adsorption (ESA); moisture-swing adsorption (MSA); membrane-based separation (m-DAC)

**Citation:** Li, G.; Yao, J. Direct Air Capture (DAC) for Achieving Net-Zero $CO_2$ Emissions: Advances, Applications, and Challenges. *Eng* **2024**, *5*, 1298–1336. https://doi.org/10.3390/eng5030069

Academic Editors: George Z. Papageorgiou, Maria Founti and George N. Nikolaidis

Received: 15 June 2024
Revised: 3 July 2024
Accepted: 3 July 2024
Published: 4 July 2024

## 1. Introduction

Greenhouse gases, especially carbon dioxide ($CO_2$), have significant impacts on global climate change, leading to rising global temperatures, rising sea levels, and increased frequency of extreme weather events [1]. These effects have brought about long-term, severe, and irreversible consequences for ecosystems and human living environments [2]. Over the past two decades, the issue of excessive $CO_2$ emissions has become increasingly significant, driven by rapid global economic development [3,4]. The global greenhouse gas emissions primarily come from four main sectors: energy (73.2%); agriculture, forestry, and land use (18.4%); industry (5.2%); and waste (3.2%) [5]. The breakdown of these categories into subcategories is illustrated in Figure 1. Energy, as a broad category contributing to the largest greenhouse gas emissions, includes subcategories such as energy used in industry (24.2%), buildings (17.5%), transport (16.2%), unallocated fuel combustion (7.8%), fugitive emissions from energy production (5.8%), and agriculture and fishing energy (1.7%) [5], all of which are closely intertwined with aspects of daily life.

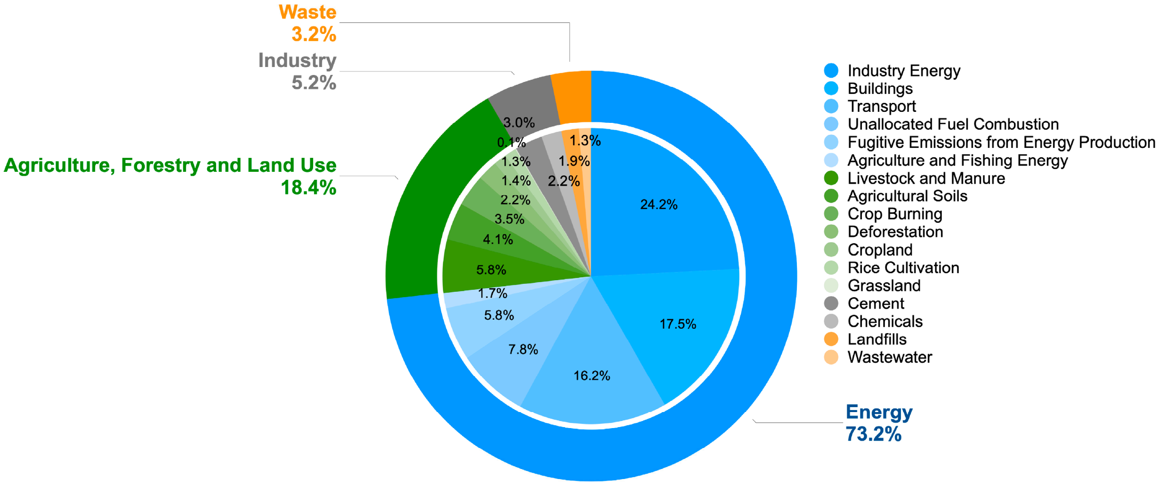

**Figure 1.** Global greenhouse gas emissions by sector. Reproduced based on data from [5] under the CC BY license.

While fossil fuels are dominant energy resources worldwide due to their availability and low cost [6–9], the production and combustion of fossil fuels are the primary causes of excessive $CO_2$ emissions, exacerbating the adverse effects of greenhouse gases [2]. Mining operations, whether for fossil fuels or other minerals and metals, typically rely heavily on machinery powered by fossil fuels for drilling, blasting, hauling, processing, and subsequent transportation. All of these processes cause direct and indirect greenhouse gas emissions, resulting in a significant carbon footprint [10,11]. To address this issue, carbon tax has been used as a method to incentivize mining industries to reduce their carbon footprint by imposing a price on carbon emissions [12]. This approach helps align economic activities with environmental goals by internalizing the costs of carbon pollution and promoting sustainable practices. The interrelation of environmental and economic factors that influence technologies to achieve production efficiency, job creation, and environmental load reduction is crucial [13,14].

The problems caused by excessive $CO_2$ emissions have gained worldwide attention. In response, the United Nations has formulated and enacted the United Nations Framework Convention on Climate Change (UNFCCC) [15]. The UNFCCC aims to establish a common political framework and cooperation platform, enabling the international community to coordinate efforts globally, collectively address climate change challenges, and promote the formulation and implementation of international climate policies. In 2015, global leaders adopted the Paris Agreement, which aims to limit the increase in global average temperature to within 2 °C above pre-industrial levels, with efforts to keep it below 1.5 °C [16]. To achieve this goal, countries have actively formulated and announced emission reduction targets and action plans.

In recent years, significant progress has been made in the development of clean energy sources such as solar power [17–19], nuclear energy [20,21], and wind power [22,23]. This has helped alleviate the issue of $CO_2$ emissions to some extent. Additionally, the promotion of carbon capture, utilization, and storage (CCUS) technology has become one of the important measures adopted by various countries to address this challenge [2,24,25]. CCUS technology primarily involves the capture and separation of $CO_2$ emitted during industrial production. Subsequently, the captured $CO_2$ is transported via pipelines or trucks and stored in designated locations for either utilization or permanent sequestration. Currently, widely used capture technologies mainly focus on capturing $CO_2$ from sources such as refineries and power plants, which typically have higher concentrations of $CO_2$, thus facilitating higher capture efficiency. However, the target of these capture techniques is limited only to high-concentration $CO_2$ emissions and requires implementation at specific emission points, making them unable to comprehensively address the issue of excess $CO_2$ in the atmosphere globally.

Direct air capture (DAC) technology, on the other hand, can overcome some of the limitations of conventional capture methods and is the most direct way to reduce carbon concentrations in the atmosphere [26,27]. Unlike conventional CCUS technologies that focus on capturing $CO_2$ from fixed emission sources, DAC facilities do not need to be connected to emission points. Therefore, they can be deployed in more locations than CCUS facilities, providing geographical flexibility and wider applicability. Additionally, DAC's deployment does not require precious arable land, thereby avoiding competition with the agriculture or bioenergy sectors for land use [26]. Moreover, DAC has the ability to capture low-concentration $CO_2$ that was released years ago but still persists in the atmosphere, making it a method to address legacy $CO_2$ emissions [2,26]. Furthermore, DAC technology can create synthetic clean fuels by combining captured carbon with clean hydrogen, enabling the production of synthetic hydrocarbon fuels [28]. These fuels, which can account for up to 40% of aviation fuel demand, can replace traditional fossil fuels such as oil, natural gas, and coal, thereby reducing greenhouse gas emissions. Therefore, DAC technology is considered by the International Energy Agency (IEA) to be one of the key technologies for achieving net-zero or negative emissions [26]. Given these significant advantages, DAC technology is poised for widespread global adoption, providing countries and regions with a universal pathway for carbon reduction and contributing to the achievement of broader carbon neutrality goals.

Given the significant impact and importance of DAC, research and application of DAC technology have become key focal points in international scientific research and efforts in recent years. According to the IEA report, to achieve a sustainable development scenario globally, it is anticipated that an average of 32 DAC plants, each capable of capturing 1 Mt $CO_2$/year, will be added annually from 2020 to 2050 [26]. However, the deployment of DAC technology still faces certain limitations. These include cost competitiveness with other mitigation measures, potential constraints on appropriate storage facilities, and limitations due to the availability of low-cost electricity and thermal energy for the continuous operation of DAC facilities. To address these challenges, governments, businesses, and research institutions worldwide are investing resources to drive innovation and development of DAC technology. Accomplishments in research related to DAC technology, spanning multiple disciplines and fields (such as materials science, chemical engineering, environmental science, and energy), have been made in improving the capture efficiency and reducing the cost of DAC technology [27,29–33]. In terms of practical application, some countries have initiated pilot DAC projects in the industrial and energy sectors [26]. Although many of these DAC projects are still small-scale, some have grown to commercial scale utilizing mature and refined DAC technology.

This study presents a comprehensive overview of DAC. It commences with an introduction to the fundamental principle of DAC, followed by an in-depth exploration of three categories of DAC technologies: liquid DAC (L-DAC), solid DAC (S-DAC), and emerging DAC technologies. Subsequently, it examines the current real-world applications of DAC technology worldwide. Building upon this foundation, this study identifies the challenges and future research directions facing DAC. The significance of this review lies in providing a comprehensive understanding of DAC technology, offering crucial information on integrated technological advancements and real-world applications to the scientific community, industry stakeholders, and policymakers. It serves as a platform for scholars worldwide to gain in-depth insights into the forefront of integrated technology. This study aims to guide global DAC technology and operations, promoting its broader adoption and contributing to the achievement of global carbon neutrality or even negative emissions targets.

## 2. Data Collection and Methodology

This study was conducted through a systematic approach encompassing literature collection, categorization, analysis, and summary. Information was sourced from a diverse range of academic research articles indexed in the Web of Science and Scopus databases, supplemented by data from the IEA, as well as relevant content from company and government reports. The timespan of the data collection ranged from 1990 to 2024. The collected information and data were systematically classified into two main categories: technological advancements, and practical applications. Each category underwent detailed analysis, subcategorization, and summarization. This methodological framework facilitated a thorough investigation of the current technological and application challenges in DAC research, enabling the identification of corresponding measures and potential future research directions.

## 3. Basic Principle of DAC

In 1999, Lackner et al. introduced the concept of extracting $CO_2$ from the air [34], which evolved into direct air capture. Their research findings confirmed the effectiveness of this technology, which utilizes atmospheric transport to convey $CO_2$ from its source to the disposal site, demonstrating its ability to control atmospheric $CO_2$ levels without limiting access to fossil energy resources. It is noteworthy that DAC technology, along with other $CO_2$ capture technologies such as pre-combustion capture, post-combustion capture, and oxy-fuel combustion capture, shares the common goal of capturing $CO_2$, but each possesses distinct applicable conditions, advantages, and disadvantages, as summarized in Table 1. Pre-combustion capture, post-combustion capture, and oxy-fuel combustion capture are typically designed for high-concentration $CO_2$ and are therefore primarily utilized in power plants [2]. In contrast, DAC technology is tailored for capturing low-concentration $CO_2$ from the atmosphere, enhancing its flexibility in deployment. However, the significant advantage of the other three capture technologies lies in their higher technological maturity compared to DAC. Moreover, they can be directly integrated into existing power plants, thereby significantly reducing initial investment costs compared to DAC. Meanwhile, DAC processes entail higher operating costs in terms of the energy and resources needed to capture equivalent amounts of $CO_2$, primarily due to the low concentration of $CO_2$ in ambient air. These technological limitations and higher costs have hindered extensive research and development of DAC since its proposal. Recently, DAC technology, as a key technology for negative carbon emissions, has gradually gained more attention. Table 2 presents several review studies summarizing research related to DAC, along with their main contents.

**Table 1.** Comparison of DAC and other $CO_2$ capture technologies [2].

| Technology | Applicability | Advantage | Disadvantage |
|---|---|---|---|
| DAC | No significant limitations | Flexible deployment options;<br>Capture of low-concentration $CO_2$;<br>Integration with renewable energy | High investment costs;<br>High operating costs;<br>Technological limitations |
| Pre-combustion capture | Integrated gasification combined cycle (IGCC) power plant | Mature technology;<br>High efficiency and easy separation | Limited applicability |
| Post-combustion capture | Pulverized coal (PC) power plant;<br>Natural gas combined cycle (NGCC) power plant;<br>Fossil fuel power plant | Mature technology;<br>Wide applicability to existing plants;<br>Retrofit application | Generation inefficiency |
| Oxy-fuel combustion capture | Pulverized coal (PC) power plant;<br>Integrated gasification combined cycle (IGCC) power plant | Mature technology;<br>High purity and concentration;<br>Simple procedures;<br>Retrofit and repowering option | High investment costs due to additional equipment required |

**Table 2.** Summary of representative review studies on DAC.

| Authors | Contents | Year | References |
|---|---|---|---|
| Bisotti et al. | This study introduces the challenges in scaling up DAC technologies from pilot to industrial scale, along with limiting factors such as the supply of critical materials and competition with the energy transition. | 2024 | [35] |
| An et al. | This study highlights the critical role of energy efficiency and regeneration energy in enabling DAC for negative emissions and discusses potential methods to lower the regeneration energy demand. | 2023 | [36] |
| Ozkan et al. | This study provides an overview of current commercial DAC technologies, highlighting the need for technological advancements to reduce costs and meet global climate goals. | 2022 | [37] |
| Erans et al. | This study explores the role of DAC as a carbon dioxide removal technology in mitigating $CO_2$ emissions, highlighting its potential alongside other negative emissions technologies and identifying research challenges across the process technology, techno-economic, and socio-political domains. | 2022 | [27] |
| Chauvy et al. | This study evaluates the environmental and economic performance of DAC through life-cycle and techno-economic assessments, highlighting potential improvements to enhance DAC's efficiency and affordability. | 2022 | [38] |
| Custelcean | This study explores the solvent-based approach to DAC, detailing its chemistry, engineering aspects, and solvent options, along with regeneration methods, to assess its potential for large-scale $CO_2$ removal. | 2022 | [31] |
| McQueen et al. | This study explores the potential of DAC using solid sorbents and liquid solvents to combat climate change, analyzing their properties and deployment considerations to enable rapid scaling and cost reduction. | 2021 | [39] |

Although the focus of these DAC-related studies varies, there is a consensus on the three stages of $CO_2$ capture in DAC: the contacting stage, the capture stage, and the separation stage, as illustrated in Figure 2. In the contacting stage, the DAC system transports atmospheric air containing $CO_2$ to the equipment using large-scale fans. Subsequently, in the $CO_2$ capture stage, $CO_2$ rapidly and effectively binds with liquid solvents in chemical reactors or solid sorbents in filters, which must possess binding energies equivalent to that of $CO_2$. Later, in the $CO_2$ separation stage, external energy sources facilitate the separation of $CO_2$ from the solvents or sorbents, yielding pure $CO_2$ and regenerated solvents or sorbents. Following the completion of these three stages, the separated pure $CO_2$ is either utilized or stored, while the recovered solvents or sorbents are recycled for reuse in the $CO_2$ capture process.

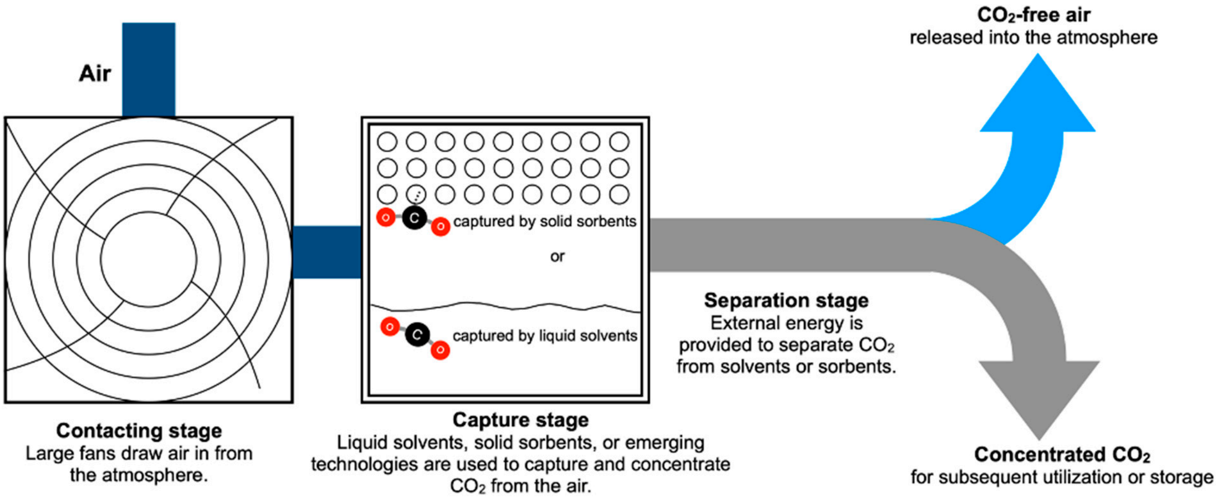

**Figure 2.** Schematic diagram of $CO_2$ capture in DAC.

It is worth noting that DAC facilities, which include large fans, reactors, filters, and separation units, rely on thermal and/or electrical energy sources for smooth operation. In recent years, to mitigate the carbon footprint of the $CO_2$ capture process and reduce dependence on fossil fuels, it has been common to select clean or renewable energy sources as the energy supply for DAC facilities. Situating DAC facilities in proximity to clean or renewable energy sources helps reduce operational costs and maximizes their carbon removal potential. Additionally, locating DAC facilities near $CO_2$ storage or utilization sites is also an option, facilitating a decrease in investments in pipeline infrastructure or fees associated with truck transportation for $CO_2$ transport, thereby concurrently lowering operational costs while reducing the risk of $CO_2$ leaks. These strategic placements optimize operational efficiency and cost-effectiveness, highlighting the potential of DAC facilities to achieve their objectives more effectively in the present era compared to their initial proposal.

Currently, liquid DAC (L-DAC) and solid DAC (S-DAC) represent two mature technologies for industrial deployment. Additionally, several emerging DAC technologies are in different stages of development, testing, or limited practical application. The following sections provide an in-depth exploration of the principles and technological advancements associated with these DAC techniques.

## 4. Liquid DAC (L-DAC)

### *4.1. Fundamental Principle of L-DAC*

L-DAC stands out as the most mature among current DAC techniques. Its fundamental principle involves the initiation of chemical reactions driven by mass transfer between specific components of the solution and atmospheric $CO_2$, resulting in the generation of specific chemical products [40,41]. Following treatment, the pure $CO_2$ and regenerated solvent can be separated to achieve continuous operation. Notably, industrial implementations of L-DAC primarily employ alkaline solutions containing KOH or NaOH [41], with occasional utilization of $Ca(OH)_2$ [42]. Figure 3 illustrates the process flow diagram, depicting two enclosed chemical loop processes.

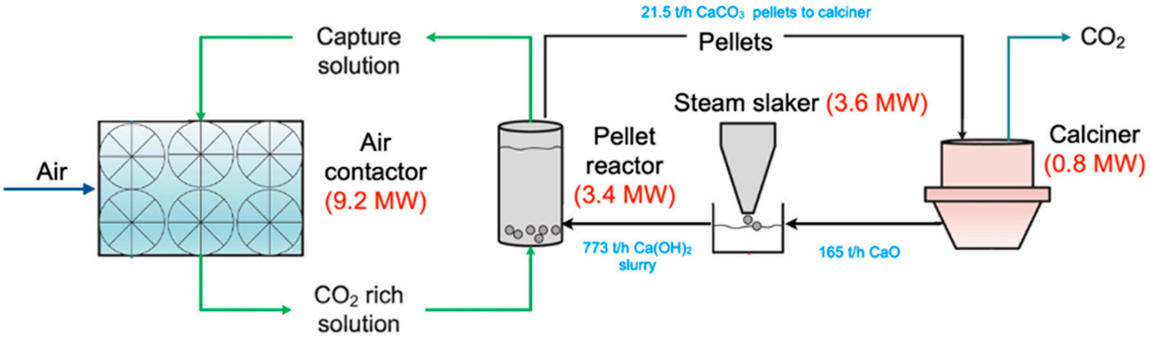

**Figure 3.** Schematic diagram of L-DAC processes. Technological parameters are indicated in blue, and electricity demands are indicated in red with the unit of megawatts (MW), both based on industry-scale conditions [41]. Reproduced with permission from [43]. Copyright 2023, Elsevier.

In the first closed loop within the air contactor, $CO_2$ is captured through contact with the solution. This process adheres to the principle of neutralization reactions between alkaline solutions and $CO_2$, resulting in the formation of carbonates. These reactions selectively interact solely with $CO_2$, effectively removing it from the air and fixing it within the solution as carbonate ions. The pertinent chemical reactions occurring during the $CO_2$ capture process in the first loop, utilizing solutions primarily composed of KOH, NaOH, and $Ca(OH)_2$, are illustrated by Reactions (1)–(3), respectively.

$$2KOH(aq) + CO_2(g) \rightarrow K_2CO_3(aq) + H_2O(l) \tag{1}$$

$$2NaOH(aq) + CO_2(g) \rightarrow Na_2CO_3(aq) + H_2O(l) \tag{2}$$

$$\mathrm{Ca(OH)_2(aq) + CO_2(g) \rightarrow CaCO_3(s) + H_2O(l)} \tag{3}$$

The second closed loop proceeds sequentially within the pellet reactor, calciner, and slaker, aiming to separate the captured $CO_2$ and recover the solvent. In this process, for solutions employing KOH and NaOH, additional chemical substances (typically $Ca(OH)_2$ in a solid slurry condition) are necessary. These substances further react with the carbonates generated in the first loop, obtaining solid calcium carbonate ($CaCO_3$). Reactions (4) and (5) illustrate these reactions for KOH and NaOH solutions, respectively. Subsequently, the separated solid calcium carbonate undergoes high-temperature heating to decompose, yielding pure $CO_2$ gas and solid calcium oxide (CaO), as depicted in Reaction (6). The solid calcium oxide further reacts with water to produce calcium hydroxide, as shown in Reaction (7), facilitating its reuse in this loop. If $Ca(OH)_2$ solution is employed in the second separation loop, there is no need to add additional substances for reactions. Instead, direct heating is utilized to achieve $CO_2$ separation and solvent regeneration, following Reactions (6) and (7). Despite offering simpler and more direct $CO_2$ capture and separation operations, $Ca(OH)_2$ solution is less commonly used due to its lower solubility in water compared to KOH and NaOH, resulting in a lower $CO_2$ capture capacity.

$$\mathrm{K_2CO_3(aq) + Ca(OH)_2(s) \rightarrow CaCO_3(s) + 2KOH(aq)} \tag{4}$$

$$\mathrm{Na_2CO_3(aq) + Ca(OH)_2(s) \rightarrow CaCO_3(s) + 2NaOH(aq)} \tag{5}$$

$$\mathrm{CaCO_3(s) \rightarrow CaO(s) + CO_2(g)} \tag{6}$$

$$\mathrm{CaO(s) + H_2O(l) \rightarrow Ca(OH)_2(s)} \tag{7}$$

### 4.2. Advantages and Disadvantages of L-DAC

The significant advantage of industrially utilized L-DAC technologies, primarily employing alkaline solutions as the principal component, lies in their ability to ensure continuous replenishment of the alkaline solution within large-scale contactors. This ensures uninterrupted and stable $CO_2$ capture processes, eliminating the need for interruptions [26]. Following $CO_2$ capture, its presence as carbonate ions within the solution facilitates its transfer to separate facilities for separation and regeneration without altering the conditions within the contactors used for capture, thus avoiding the need for cycling conditions within large-scale air contactors.

Capturing $CO_2$ at room temperature or with minimal temperature increase is generally ideal, as it significantly reduces the energy consumption and costs associated with using fuel to produce heat. However, in the L-DAC process, it is necessary to use natural gas combustion to increase the operating temperature, which represents a significant disadvantage of this technology. Specifically, the reactions occurring in the air contactor and pellet reactor are completed at approximately 20 °C. In contrast, the reactions in the calciner and steam slaker require higher operating temperatures based on reaction thermodynamics and pilot data [41]. The calciner's operating temperature needs to reach 900 °C, while the steam slaker requires an operating temperature of 300 °C. These high temperature requirements, along with the need for additional water sources for continuous solvent regeneration, increase the operational costs of L-DAC, representing a notable drawback. Additionally, due to the corrosive nature of strong alkaline solutions, equipment used in L-DAC typically requires corrosion-resistant materials such as stainless steels, nickel alloys, or specialized coatings capable of withstanding alkaline corrosion [44–46]. Implementing a rigorous maintenance schedule to regularly inspect equipment for signs of corrosion and wear is also essential to ensure longevity and reliability. These requirements underscore the heightened demands placed on equipment in L-DAC technology.

### *4.3. Technological Advancements of L-DAC*

#### 4.3.1. Advances in L-DAC Utilizing Alkaline Solutions

As the most mature DAC technology, L-DAC utilizing alkaline solutions has been commercially deployed on a large scale in several countries [40]. Recent significant advancements in this technology have focused on enhancing commercial-scale projects based on practical application scenarios. These advancements aim to achieve high capture efficiency while also controlling engineering costs to ensure the economic feasibility of L-DAC projects.

The efficiency of $CO_2$ capture in L-DAC utilizing alkaline solutions is determined by the process occurring in the first loop within the contactor. In this loop, the alkaline solution flows vertically from top to bottom, while $CO_2$ gas flows horizontally, perpendicular to the solution flow direction, creating a cross-flow pattern [47]. This pattern ensures efficient contact at the liquid surface, facilitating the capture of $CO_2$ from the air on the thin film of the solution. The efficiency of $CO_2$ capture is controlled by the diffusion of $CO_2$ molecules into the solution and their subsequent reaction with the chemical substances in the solution [41]. Consequently, optimizing the diffusion and reaction processes has been a primary focus of recent advancements.

The optimization of the contactor is primarily based on core engineering constraints, ensuring that the design can efficiently bring large quantities of ambient air into contact with fluids. On this basis, Holmes and Keith proposed using a cost optimization model to evaluate cost trade-offs and determine optimal parameters, thus maximizing economic feasibility [47]. With the goal of capturing 1 $MtCO_2$/year, they optimized the contactor structure and relevant parameters to effectively accelerate the diffusion and reaction processes of $CO_2$. A simplified schematic of the air contactor's structure is shown in Figure 4. It resembles industrial cooling towers [47,48], incorporating fans, structured packing, demisters, fluid distribution systems, and fiber-reinforced plastic structural components. The structured packing serves as a medium, with a large surface area to facilitate efficient contact between the air and a thin solution film for $CO_2$ capture. Therefore, optimizing the structured packing to absorb a significant portion of $CO_2$ from the air by minimizing frictional air resistance, while maintaining a low pressure drop to minimize the fan energy requirements at high air throughputs, is crucial for efficient $CO_2$ diffusion and reaction processes. To achieve this, the structured packing's air travel depth was optimized from the original 2–3 m to 7 m [41], significantly enhancing the contact efficiency between the solvent and air within the structured packing. Subsequent collaborative research by Grace et al. affirmed that, paired with the designed air velocity of 1.4 m/s, the optimized structured packing exhibited a pressure drop of 9.7 Pa/m during capture operations, notably reduced by over 30%, thereby decreasing the energy consumption [41].

In addition to the contactor's structure, the efficiency of $CO_2$ capture is influenced by the mass transfer coefficient of $CO_2$ and the liquid-to-gas volumetric flow ratio. The mass transfer coefficient of $CO_2$ determines the rate at which $CO_2$ is transferred from the gas phase to the liquid phase during diffusion, primarily influenced by the concentration of hydroxide ions ($OH^-$) and the temperature of the solution. For well-wetted structured packing in industrial plants, Keith et al. estimated the mass transfer coefficient of $CO_2$ to be approximately 1.3 mm/s under typical operating temperatures (20 °C), using a combination of semi-empirical formulae, empirical data, and modeling methods, with a typical solution composition of 1.0 M $OH^-$ [41]. The liquid-to-gas volumetric flow ratio refers to the relative ratio of the liquid-phase volumetric flow rate to the gas-phase volumetric flow rate [49], describing their proportions within the contactor. Typically, a lower ratio, indicating less liquid per unit of gas, favors more thorough gas contact within the packing in the lower liquid flow regime, thereby enhancing the capture efficiency. Additionally, a reduced liquid-to-gas volumetric flow ratio signifies lower energy consumption for liquid pumping to achieve a low liquid flow rate, thereby mitigating energy costs to a certain extent [47]. However, it is crucial to note that excessively low liquid flow rates may lead to incomplete wetting of the packing, impeding effective gas–liquid contact for reaction and capture, consequently diminishing the capture efficiency. Therefore, selecting well-wetted packing while minimizing energy consumption is paramount. Addressing these requisites, Holmes and Keith proposed a method involving periodic alternation of liquid flow rates [47]. This approach employs short cycles of high liquid flow to ensure adequate wetting of the packing material and remove dust and debris, along with long cycles of low liquid flow for cost-effective and efficient $CO_2$ capture [47]. Furthermore, the gas volumetric flow rate is determined by multiplying the air flow rate by the inlet area. It is important to note that higher air velocities increase energy consumption, which is a primary contributor to operating costs. Simultaneously, higher air rates minimize the required contactor inlet area, thereby diminishing the contribution of capital costs per unit of $CO_2$ captured. Consequently, ascertaining the optimal air rate is pivotal to minimizing combined energy and capital costs. Given the multifaceted fluid dynamics involved in L-DAC, encompassing flow, diffusion, mass transfer, and reactions between liquids and gases, recent research has advocated employing computational fluid dynamics simulations in tandem with cost optimization models [29,48,50,51]. This integrated approach facilitates the determination of critical gas–liquid fluid parameters and equipment geometric parameters, thus serving as a requisite and efficacious means to enhance $CO_2$ capture efficiency while ensuring economic viability.

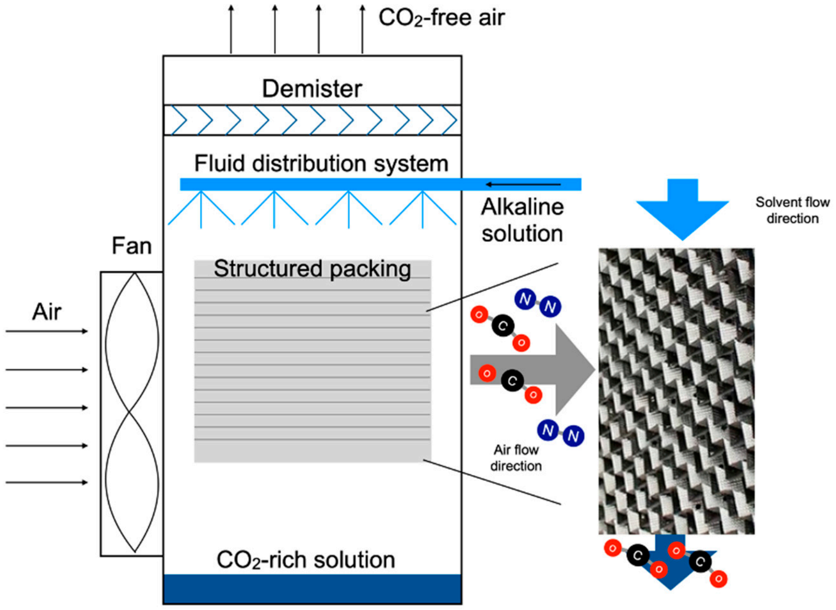

**Figure 4.** Simplified schematic of the air contactor structure used in L-DAC technology.

Advancements in L-DAC separation and recovery technologies have primarily focused on enhancing the operational efficiency and improving essential equipment such as the pellet reactor, calciner, and slaker. Notably, within the pellet reactor, where carbonate precipitation occurs, significant strides have been made towards reducing separation costs. Keith et al. proposed that precipitating $CaCO_3$ in the form of small pellets, as opposed to lime mud, offers distinct advantages for subsequent washing and drying processes, thereby lowering the overall processing costs [41]. Consequently, a key strategy employed in the pellet reactor involves the simultaneous injection of $Ca(OH)_2$ slurry alongside additional 0.1–0.9 mm $CaCO_3$ pellets, which act as seed pellets. Initially, these seed pellets, due to their small size and light weight, remain suspended within the solution. As the continuous reaction between $Ca(OH)_2$ and carbonate ions progresses, $CaCO_3$ precipitates gradually form. Leveraging the high surface area provided by the seed pellets, the $CaCO_3$ precipitate preferentially adheres to them, leading to their continual accumulation and growth. Ultimately, as the $CaCO_3$ pellets reach a critical mass, they settle at the bottom of the reactor, facilitating the solid separation of $CaCO_3$ for subsequent processing steps. It is worth noting that using KOH instead of NaOH in the pellet reactor offers significant advantages [41]. When capturing $CO_2$ using these two solutions, the resulting products are $K_2CO_3$ and $Na_2CO_3$, respectively. $K_2CO_3$ exhibits significantly higher solubility, with approximately 110 g of $K_2CO_3$ dissolving per 100 g of water at 20 °C, compared to only 20 g of $Na_2CO_3$. This solubility difference results in a higher concentration of carbonate ions in the $K_2CO_3$ solution, enhancing the reaction rate for $CaCO_3$ formation. Consequently, KOH usage increases the carbonate concentration, enhancing $Ca(OH)_2$ utilization and reducing the required amount of $Ca(OH)_2$. This reduces raw material costs while enhancing the reaction efficiency and yield, making it more economically competitive.

In the calciner, advancements in $CO_2$ regeneration focus on improving energy efficiency and system reliability [41]. By utilizing a conservative heat integration design and two counter-current heat recovery cyclone separators, the system efficiently lowers the exit gas temperature from 900 °C to 650 °C, and then to the target temperature of 325 °C, while heating the incoming solids. The incoming solids are preheated to 450 °C and, further, to 650 °C. This design integrates solid particle preheating, gas cooling, and steam generation, using the cooling gas to preheat the solids. It also mitigates the risk associated with large temperature fluctuations, maximizing energy efficiency and system reliability.

Significant technological advancements have been made in optimizing thermodynamic properties in the process of regenerating $Ca(OH)_2$ slurry from CaO in the slaker. Traditionally, water slakers were commonly used for the slaking reaction, but due to the boiling point limitation of water, the heat released during the slaking reaction could not be fully utilized at higher temperatures, leading to energy waste. To address this issue, steam slakers have been proposed as a replacement for water slakers [41]. The advantage of using steam lies in its higher temperature range, allowing the heat released from the slaking reaction to be fully utilized at elevated temperatures. In this improved technology, the steam slaker employs a recirculating steam flow to transport and slake quicklime (CaO) particles to form $Ca(OH)_2$, which is subsequently collected in a dust collector. The outgoing stream from the steam slaker contains significant heat, including that generated by the slaking reaction, which can be used to dry and warm the $CaCO_3$ pellets from the pellet reactor, thereby maximizing the utilization of the released heat.

#### 4.3.2. Advances in L-DAC Utilizing Other Liquid Solvents

In addition to the current industrialized L-DAC technology that uses alkaline solutions, research has focused on other liquid solvents. Typical liquid solvents used in traditional $CO_2$ capture processes during post-combustion, pre-combustion, and oxy-fuel combustion, such as amine-based solvents and ionic liquids (ILs), have shown potential for application in L-DAC [52].

Various amine-based solvents, including chilled ammonia [53–55], low-volatility aminosilicones [56–58], monoethanolamine (MEA) [59–62], and N-methyldiethanolamine (MDEA) [63–66], utilize their amine groups to react with $CO_2$, forming products such as carbamates or bicarbonates [67]. These products can dissolve in the solvent, enabling the absorption and capture of $CO_2$, which can then be released through heating. However, it is important to note that the chemical reactions occurring during the capture of $CO_2$ by amine-based solvents involve a large enthalpy [68], necessitating additional heat input to regenerate the amine-based solvents during $CO_2$ release [69], leading to increased energy consumption. Additionally, some byproducts generated during the chemical reactions of amine-based solvents in the DAC process, such as aerosols [70–72] and nitrosamines [73–75], may be toxic and carcinogenic. Considering these drawbacks, amine-based solvents are not ideal materials for large-scale practical application in L-DAC.

Recent research suggests that ILs hold promise as solvents for L-DAC due to their high thermal stability and tunability. ILs are custom-designed salts composed of ions [52], with $CO_2$ selectivity and capacity being crucial characteristics for ILs to facilitate $CO_2$ capture and separation [67]. The capture of $CO_2$ by ILs is achieved through chemical and/or physical absorption [76]. Subsequently, $CO_2$ can be released, and the ILs can be recycled for reuse through depressurization or heating methods.

Physical absorption represents the primary mechanism for $CO_2$ capture by ILs. Ramdin et al. indicated that while ILs exhibit various intermolecular interactions, including electrostatic forces, hydrogen bonding, and van der Waals forces, the attractive van der Waals forces predominantly govern the dissolution behavior of $CO_2$, serving as the primary mechanism for $CO_2$ capture in ILs [69]. This is followed by electrostatic interactions, whereas hydrogen bonds play a negligible role [77]. Additionally, the free volume mechanism, where $CO_2$ molecules are accommodated in the free spaces of the liquid, represents another mechanism for the physical absorption of $CO_2$ by ILs [78]. Beyond these detailed discussions on the mechanisms, comparative studies have been conducted on the effects of common cations such as imidazolium, pyrrolidinium, pyridinium, guanidinium, phosphonium, and morpholinium, as well as common anions such as hexafluorophosphate, tetrafluoroborate, alkylsulfate, triflate, and dicyanamide, on $CO_2$ capture efficiency in ILs [69]. These studies clearly demonstrate that the anion is the primary factor influencing $CO_2$ dissolution in ILs, while the cation plays a secondary role [79–81]. Furthermore, ILs with fluorination structures have been shown to significantly enhance the solubility of $CO_2$ in ILs, with anion fluorination exhibiting a more significant improvement compared to cation fluorination [82]. Additionally, longer alkyl chains on cations can also enhance the solubility of $CO_2$ in ILs to some extent [69].

Chemical absorption of $CO_2$ by ILs builds upon their physical absorption capability by leveraging suitable functional groups, such as amino acids, to initiate chemical reactions with $CO_2$. This maintains or enhances $CO_2$ selectivity while significantly increasing the capacity [67]. Studies have shown that the enhancement of ILs' properties can be achieved by incorporating specific functional groups [67]. Integrating a free amine functional group into the alkyl chain of an imidazolium cation within an IL has been demonstrated to induce chemical complexation, thereby enhancing the $CO_2$ capture capacity [83]. ILs modified in this manner, known as amino-acid-based ILs [67], have shown significantly enhanced $CO_2$ capacity on a molar basis [67,84]. The choice of functional groups near the amine can influence the reaction heat and, consequently, the energy required to separate $CO_2$ from the solvent. Incorporating electron-withdrawing or electron-donating groups may mitigate the reaction heat to some extent [67].

Recent progress in the study of ILs for $CO_2$ capture has been primarily directed towards enhancing their physical and chemical properties by optimizing the combination of different cations and anions. Elmobarak et al. conducted a comprehensive review of recent developments in ILs for $CO_2$ capture by comparing several ILs used for $CO_2$ capture based on their physical characteristics, including solubility, selectivity, viscosity, and volatility [52]. Furthermore, simulations are considered to be a valuable method for assessing the properties of ILs before synthesizing optimal variants, thus enabling cost-effective optimization [85–87].

In addition, recent studies have explored the use of amino acid salt (AAS) solutions [88–90], which can be synthesized from ILs, strong inorganic alkalis, organic amines, and activators, for $CO_2$ capture [91]. Zhang et al. conducted a comprehensive review on the effectiveness of AAS solutions in capturing $CO_2$, extensively elaborating on the thermodynamic and kinetic properties of various AAS solutions applicable for $CO_2$ capture, and comparing their performance in absorption and regeneration processes [91]. This provides valuable insights for enhancing the efficiency of $CO_2$ capture using AAS solutions.

## 5. Solid DAC (S-DAC)

### *5.1. Fundamental Principle of S-DAC*

The core principle of S-DAC technology involves using solid sorbents to capture $CO_2$ from ambient air at room temperature and atmospheric pressure. Subsequently, $CO_2$ is released from the sorbents under low pressure and moderate temperatures (80–100 °C) through a temperature-vacuum swing process. The process flow of this technology is illustrated in Figure 5.

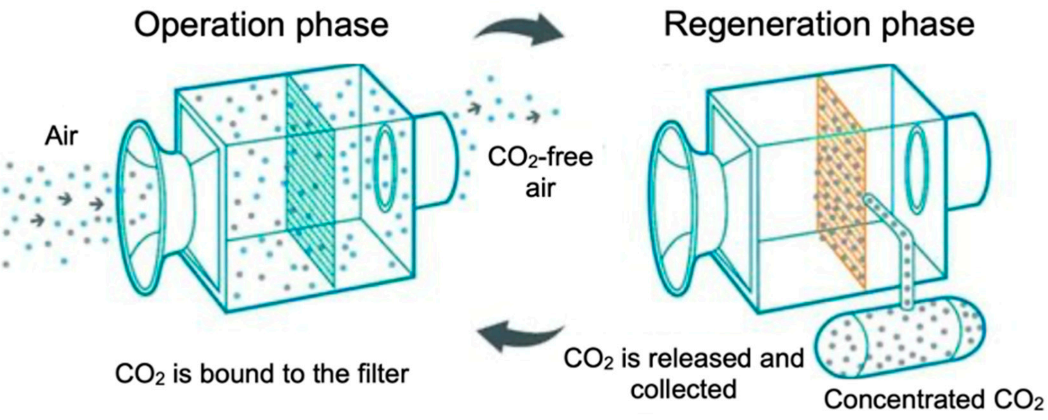

**Figure 5.** Schematic diagram of S-DAC's process flow. Reproduced with permission from [92] under the CC BY license.

In the current industrial application of S-DAC, the primary solid sorbents utilized are alkaline-functionalized sorbents [92], which are materials with alkaline functional groups such as amine groups [93], hydroxyl groups [93], quaternary ammonium groups [94], and piperidine groups [95]. The primary principle of these sorbents for capturing $CO_2$ is acid–base reaction, supported by their high surface areas and porous structures, which enhance their $CO_2$ adsorption capacities. Particularly, amine-based sorbents, where amine compounds ($RNH_2$) are bonded to filter materials composed of dry porous granulates, are widely employed in S-DAC [24]. The high chemical reactivity, thermodynamic properties, and long-term stability of amine groups under ultralow $CO_2$ concentration conditions make them particularly effective for capturing $CO_2$ molecules [24]. These sorbents fix $CO_2$ at ambient temperatures and, upon heating to the temperature range of 80–100 °C, the increased thermal energy facilitates the release of $CO_2$ from the sorbents. Filter materials support and maintain the solid sorbents, and their porous structure allows air to pass through for adsorption. In S-DAC plants, fans draw air into collectors, where amine-based solid sorbents bind $CO_2$, forming carbamate compounds through amination reactions. The reaction products depend on the presence of water in the system. In the absence of water, the products include ammonium carbamate ions and paired carbamic acid [30]. In the presence of water, the products include ammonium bicarbonate and water-stabilized carbamic acid [30]. This process fixes $CO_2$, concentrating it on the filter, while $CO_2$-free air is expelled from the collector. Once the solid sorbent is saturated with $CO_2$, the adsorption process ends, and the collector is sealed and heated to desorb $CO_2$. During this desorption process, the solid sorbent regenerates and regains its adsorption capacity, while pure $CO_2$ gas is released. This cyclic process of adsorption and desorption enables the continuous capture of $CO_2$ from the air and the release of pure $CO_2$.

### 5.2. Advantages and Disadvantages of S-DAC

The current industrial-scale S-DAC technology offers advantages such as low energy consumption, low operating costs, and suitability for a wide range of scales. Specifically, compared to L-DAC, which may require temperatures as high as 900 °C for desorption, solid sorbents typically only need temperatures in the range of 80–100 °C, resulting in lower energy consumption and operating costs. Additionally, S-DAC technology operates in a small-scale modular mode, allowing scalability based on the needs of various application scenarios, from small laboratory setups to large industrial implementations [26]. This flexibility makes S-DAC a versatile solution for different $CO_2$ capture applications. Furthermore, S-DAC can extract water from the air during the capture process, eliminating the need for an additional water supply.

The disadvantages of current S-DAC facilities primarily include high construction costs and the sustainability of sorbents. S-DAC relies on batch operations, requiring multiple units to be operated in parallel, resulting in larger, more complex plant structures and increased construction costs [26]. Additionally, the regeneration step in S-DAC necessitates periodic sealing of the entire structure from ambient air, along with cycling temperature, pressure-vacuum conditions, or humidity. These specific construction requirements further increase costs. Additionally, the solid sorbents are required to withstand prolonged exposure to impure environments without experiencing premature degradation or failure in capturing $CO_2$. This necessitates regular replacement of the sorbents, thereby further increasing the operational costs [26,41].

### *5.3. Technological Advancements of S-DAC*

In recent years, the optimization of solid sorbent materials has emerged as a primary advancement in S-DAC technology, aimed at enhancing the efficiency of $CO_2$ capture from ambient air. Current research endeavors primarily focus on two key areas: the optimization of amine-based sorbents, and the utilization of porous materials with microscale-to-macroscale pores or voids.

#### 5.3.1. Advances in Amine-Based Sorbents

Recent optimization studies on amine-based solid sorbents have primarily focused on enhancing their adsorption performance by tethering or immobilizing them onto other supporting materials to form amine-modified sorbents [96].

In determining suitable basic amines for S-DAC technology, Heydari-Gorji et al. [97] and Sayari et al. [96] conducted thorough investigations into various types of amine compounds featuring different amine groups and molecular structures, focusing on aspects such as $CO_2$ uptake capacity and stability. Their research confirmed that primary, secondary, and tertiary monoamines all exhibit decomposition at specific temperatures, and the decrease in $CO_2$ uptake was attributed to the formation of urea linkages at the expense of amine groups [96]. The chemical structures of the basic amines commonly used for DAC are depicted in Figure 6. Polyethyleneimine (PEI) is considered to be a more suitable amine-based sorbent due to its structure containing high-temperature-stable monoamines [98], compared to other polyamine materials such as poly(allylamine) (PAA) [99,100], poly(glycidyl amine) (PGA) [101], poly(propylene guanidine) (PPG) [102,103], and tetraethylenepentamine (TEPA) [104,105].

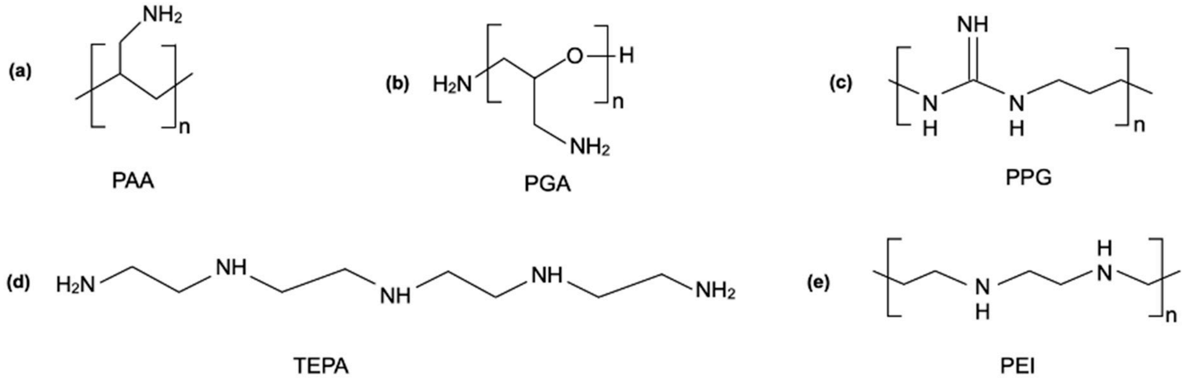

**Figure 6.** Chemical structures of commonly employed amines for S-DAC: (**a**) poly(allylamine) (PAA); (**b**) poly(glycidyl amine) (PGA); (**c**) poly(propylene guanidine) (PPG); (**d**) tetraethylenepentamine (TEPA); (**e**) polyethyleneimine (PEI).

To further optimize the $CO_2$ capture performance of PEI, recent studies have focused on PEI-modified sorbents, a typical class of amine-modified sorbents [106–108]. These studies involved chemically modifying the basic structure of PEI. Significant progress has been made in utilizing silica supports to form PEI-based aminosilica materials, also referred to as silica-polyethyleneimine materials. Choi et al. proposed modifying PEI with (3-aminopropyl)trimethoxysilane (Figure 7a) to form A-PEI/silica, and with tetraethyl orthotitanate (Figure 7b) to form T-PEI/silica. Their research confirmed that these modified PEI-based aminosilica sorbents exhibit enhanced adsorption kinetics, higher $CO_2$ adsorption capacities, and greater thermal stability compared to the original PEI. This improvement was attributed to the increased density of amine groups, stronger chemical bonds and interactions, and enhanced surface area and porosity [98]. Sayari et al. proposed loading PEI onto PME (pore-expanded MCM-41e), a silica support with internal surfaces fully covered by a uniform layer of readily accessible long alkyl chains from cetyltrimethylammonium (CTMA+) cations [109]. This PEI/PME material benefits from PME's larger pore volume and surface area. Furthermore, PME serves as an excellent support due to the enhanced dispersion of PEI within the surface layer, which increases the accessibility of amine groups and improves mass transport [109,110]. These properties result in significantly enhanced $CO_2$ capture performance for this material. Miao et al. introduced and synthesized a novel material, DEA/PEI, through the incorporation of diethanolamine (DEA) into polyethyleneimine (PEI) [106], with the molecular structure of DEA depicted in Figure 7c. This new material fully utilizes the synergistic effect between DEA and PEI to enhance $CO_2$ capture capacity [106]. Specifically, in addition to exhibiting properties of larger pore volume, DEA's hydroxyl groups facilitate increased accessibility between $CO_2$ and amines while stabilizing the carbamate anion through hydrogen bonding. Additionally, the incorporation of DEA reduces the viscosity of PEI, thereby mitigating PEI's agglomeration. Furthermore, the appropriate addition of DEA to PEI significantly extends the adsorption period, with a high adsorption rate, leading to enhanced $CO_2$ capacities and amine efficiency [106]. The optimization of this DEA/PEI "mixed amine" system provides practical support for S-DAC applications.

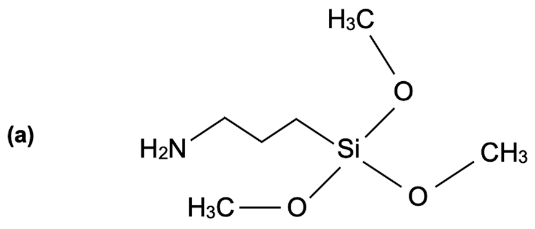

(3-Aminopropyl)trimethoxysilane

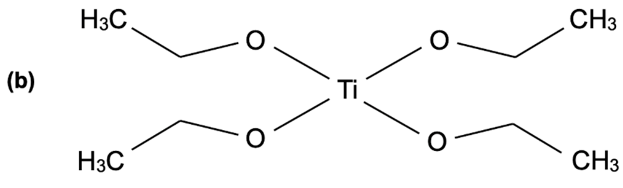

Tetraethyl orthotitanate

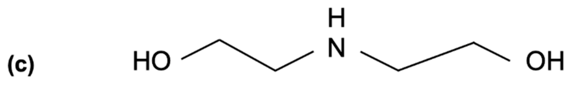

DEA

**Figure 7.** Molecular structures of some support materials used in synthesizing PEI-modified sorbents: (**a**) (3-aminopropyl)trimethoxysilane; (**b**) tetraethyl orthotitanate; (**c**) diethanolamine (DEA).

#### 5.3.2. Advances in Porous Material Sorbents

The significant advantages of using porous materials for $CO_2$ capture include their cleanliness, reversibility, and low energy demand [40]. Typically, these materials rely mainly on physisorption, primarily governed by van der Waals forces, although chemisorption may occasionally contribute to $CO_2$ capture and separation. A wide range of porous materials have been studied for their potential application in S-DAC.

Some porous materials utilize their inherent pore structures for $CO_2$ capture, exemplified by activated carbon (AC) [111–113], carbon-based materials (CBMs) [111,114,115], zeolites [111,116–118], boron nitride (BN) nanomaterials [119–121], and porous silica materials [122,123]. Chue et al. discussed the adsorption mechanisms and performance of AC, carbon molecular sieves (CMSs), and zeolites for $CO_2$ capture [111]. AC primarily adsorbs $CO_2$ onto its porous surface due to its high selectivity for $CO_2$. CMSs, derived from CBMs, selectively adsorb $CO_2$ based on pore size and polarity. Zeolites, which are aluminosilicate minerals, capture $CO_2$ due to their adsorption capacities and higher selectivity for $CO_2$ over $N_2$. Abd et al. conducted a comprehensive review of recent advancements in ACs sourced from various origins for $CO_2$ capture, emphasizing that surface modifications of these ACs can further enhance their adsorption performance [124]. Zaker et al. extensively explored CBMs as suitable candidates for $CO_2$ capture, attributed to their cost efficiency, easy regeneration, and robust adsorption capacities for significant amounts of $CO_2$ [125]. They provided detailed insights into the production, modification, and performance of CBMs, with a mechanism of $CO_2$ capture by CBMs depicted in Figure 8a. Kumar et al. conducted a comprehensive analysis of the advancements and future prospects of zeolites as sorbents for $CO_2$ capture, highlighting the significant potential of zeolites in this regard [116]. Their high porosity, ultra-small pores, structural diversity, stability, recyclability, and chemical reactivity contribute to their efficacy. A schematic illustration depicting $CO_2$ capture by zeolites is presented in Figure 8b. Sun et al. demonstrated that porous BN nanomaterials, including BN nanosheets, nanotubes, and nanofibers, can achieve $CO_2$ capture and release by simply controlling the charges carried by BN nanomaterials [119]. The schematic illustration of $CO_2$ capture by BN nanomaterials is depicted in Figure 8c. Subsequently, Liang et al. proposed the utilization of Cu-loaded BN nanofibers, which exhibit significantly enhanced $CO_2$ adsorption capacity and high recyclability for repeated uses compared to BN nanofibers [120]. This enhancement can be attributed to Cu's ability to modulate electron transfer between porous BN and $CO_2$, as illustrated in Figure 8d. Porous silica materials, characterized by highly ordered pore structures, high surface area, high pore volume, tunable pore size, and good thermal and mechanical stability, are also regarded as suitable candidates for $CO_2$ capture. Amaraweera et al. conducted a comprehensive review of $CO_2$ capture using porous silica materials, detailing various synthesis protocols for different types of mesoporous silica with diverse pore geometries, as well as other significant applications of these porous silica materials beyond $CO_2$ capture [122].

In addition to the aforementioned materials with inherent porous structures, there has been a recent increase in the synthesis of materials specifically designed to have porous structures. These include metal–organic frameworks (MOFs) [126–128], covalent organic frameworks (COFs) [40,129,130], porous organic polymers (POPs) [131], porous aromatic frameworks (PAFs) [132,133], and polymers of intrinsic microporosity (PIMs) [134,135]. These materials share common characteristics, such as high porosity, high surface area, and structural tunability, making them promising solid sorbents for DAC applications.

MOFs are a class of hybrid porous materials, formed by tuning the type and arrangement of organic ligands and metal centers to create optimized pore structures and surface properties [126], as illustrated in Figure 9a. Ghanbari et al. conducted a comprehensive analysis of MOFs suitable for $CO_2$ capture, detailing the mechanisms of $CO_2$ selectivity over other gases, the preparation and synthesis methods of MOFs, and strategies to enhance $CO_2$ adsorption on MOFs [126]. MOFs leverage their robust 3D permanent porous structure, extraordinary surface area, surface functionality, and modular nature to achieve $CO_2$ separation and capture. The process of separating $CO_2$ from air using MOFs is depicted in Figure 9b. When air passes through MOFs, several effects may contribute to the $CO_2$ capture process. Among these, the molecular sieving effect is significant, wherein molecules with kinetic diameters matching the pore sizes of MOFs exhibit the highest affinity for the materials. $CO_2$, with a kinetic diameter of 3.3 Å, aligns with the pore diameter of MOFs, enhancing its likelihood of capture within the pores compared to nitrogen [126,127]. Furthermore, the kinetic or thermodynamic equilibrium effect [128] is also significant. This effect arises from $CO_2$'s large quadrupole moment, which, in contrast to the nonpolar nature of $N_2$ molecules, enables the selective adsorption of $CO_2$ by MOFs [126,128]. Furthermore, the presence of functional groups in the framework, such as polar groups [136,137], $\pi$-electrons [138], and coordinatively unsaturated metal sites [139,140], further enhances the interaction with $CO_2$, promoting greater adsorption over other gas components [126].

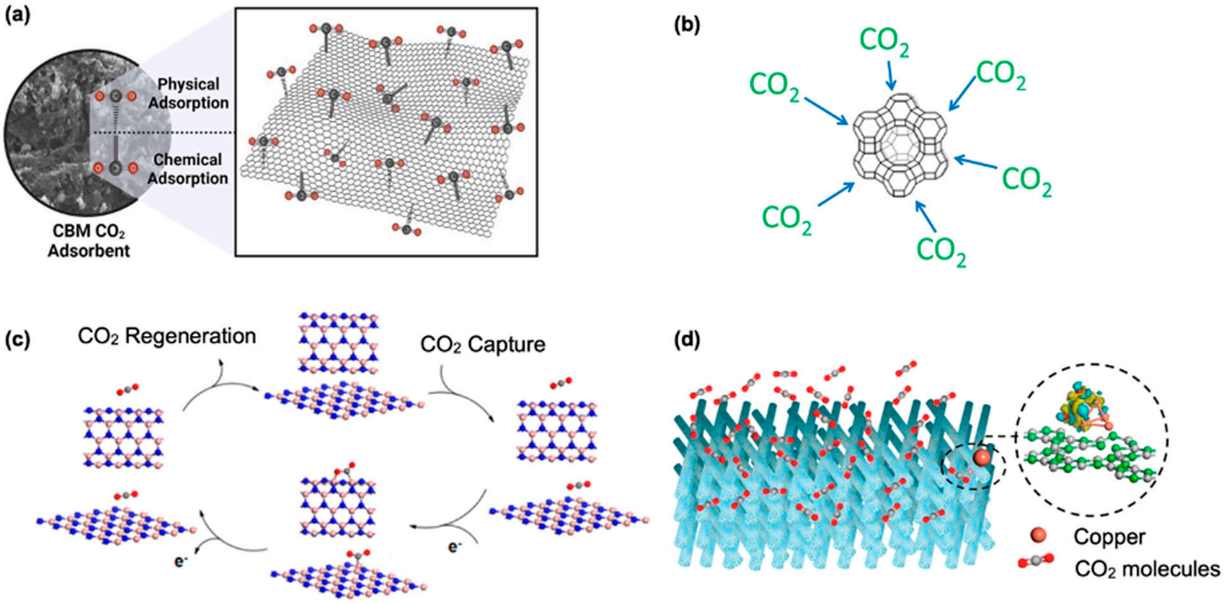

**Figure 8.** Mechanistic illustration of $CO_2$ capture by some materials with inherent pore structures: (**a**) $CO_2$ capture by CBMs. Reprinted with permission from [125]. Copyright 2023, Elsevier. (**b**) $CO_2$ capture by zeolites. Reprinted with permission from [116]. Copyright 2020, Elsevier. (**c**) $CO_2$ capture by boron nitride nanomaterials. Reproduced with permission from [119]. Copyright 2013, American Chemical Society. (**d**) $CO_2$ capture by Cu-loaded porous boron nitride nanofibers. Reproduced with permission from [120]. Copyright 2020, American Chemical Society.

COFs are porous materials composed of organic units connected by covalent bonds, characterized by highly ordered crystalline structures with adjustable pore size and morphology, high surface areas, and low density [141]. They are considered to be suitable candidates for $CO_2$ capture as well as other applications [129,141–144], such as proton-conducting electrolytes, catalysis, and drug delivery. Li et al. conducted a review on COFs for $CO_2$ capture, focusing on fabricating COFs to enhance $CO_2$ capture efficiency [40]. They emphasized the vital role of COFs' affinity for $CO_2$, particularly under low-$CO_2$-concentration conditions in DAC. Therefore, introducing $CO_2$ affinity units such as -OH, -COOH, and -$NH_2$ into COFs' pores, either through covalent incorporation or physical loading, is an effective approach to increase $CO_2$ uptake capacities [40,145]. Notably, Lyu et al. pioneered the covalent incorporation of amines into COFs [130]. In their study, they synthesized a novel material named COF-609, featuring a base-stable tetrahydroquinoline linkage covalently bonded to tris(3-aminopropyl)amine, the chemical structure and $CO_2$ capture mechanism of which are depicted in Figure 10. This optimized material not only offers sufficient pore space to increase the contact area with $CO_2$ but also enhances polarity and introduces a secondary amine into the structure, enabling strong chemisorption of $CO_2$.

This material achieves a 1360-fold increase in uptake capacity compared to the original framework for $CO_2$ capture from dry air [130].

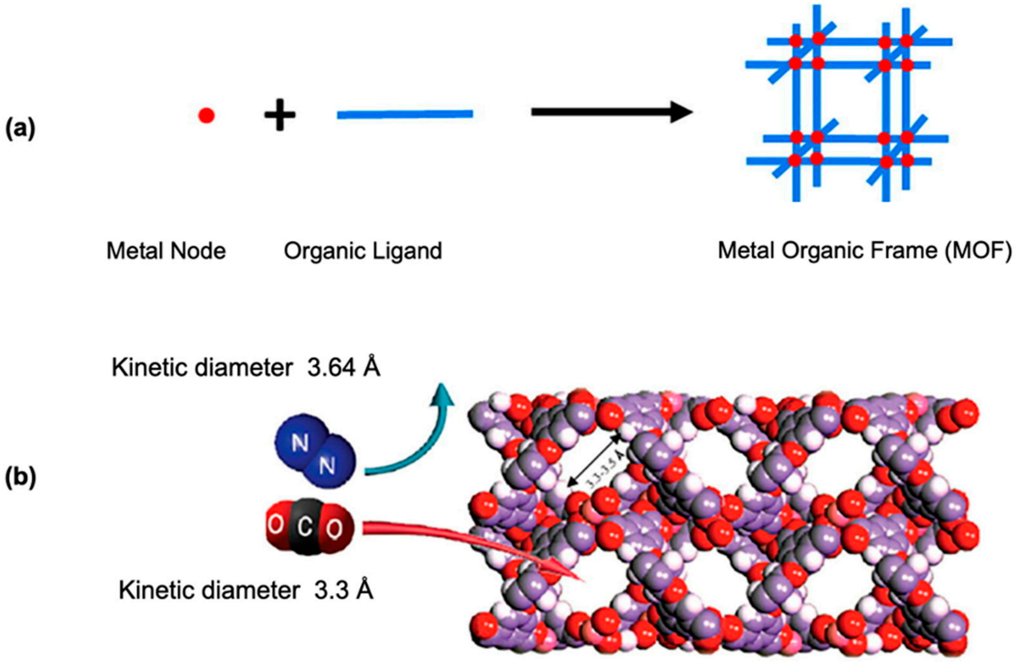

**Figure 9.** Schematic diagram of MOFs' formation and $CO_2$ capture mechanism: (**a**) Formation of MOF. (**b**) Selective gas adsorption in MOFs. Reprinted with permission from [126]. Copyright 2020, Elsevier.

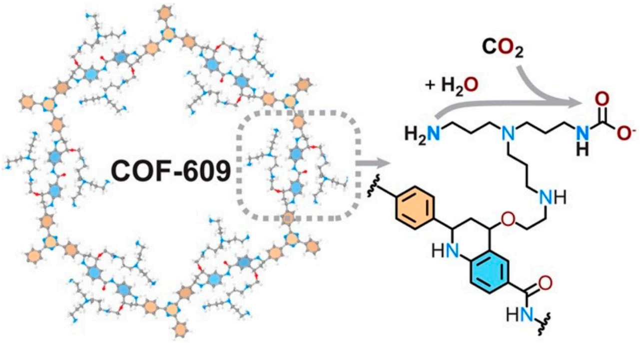

**Figure 10.** Schematic diagram of COF-609 chemical structure and its $CO_2$ capture mechanism. Reprinted with permission from [130]. Copyright 2022, American Chemical Society.

POPs, as amorphous porous materials, may not have the ideal structural crystallinity of MOFs and COFs; however, their simplicity of synthesis and low cost make them attractive candidates for large-scale, economical production as solid $CO_2$ sorbents [131]. By using suitable functionalized precursors, the desired functionalities of POPs can be easily adjusted [146]. Different synthesis strategies allow for the incorporation of building blocks such as molecular cages and macrocycles, enabling diverse structures of POPs for complex gas separation tasks [147,148]. Additionally, POPs can act as hosts or directly as heterogeneous catalysts, achieving $CO_2$ capture and conversion simultaneously [131]. Recent studies indicate that incorporating dispersed metal ion catalytic sites, single-atom catalysts (SACs), or nanoparticles such as Al, Zn, Co, Pd, Ir, Ru, and Ni into POPs, forming metal-containing POPs, can further enhance the functionality of heteroatoms within POPs [131,149]. This effectively creates stable, high-affinity binding sites and catalytic sites for $CO_2$, thereby improving the $CO_2$ adsorption and conversion performance of POPs. Song et al. provided profound and comprehensive insights into the significant impacts of different POPs' structures and properties on $CO_2$ capture, separation, and conversion processes [131]. The schematic illustration of the design principles of POPs for $CO_2$ capture and separation, along with the subsequent conversion of $CO_2$ into value-added products, is shown in Figure 11.

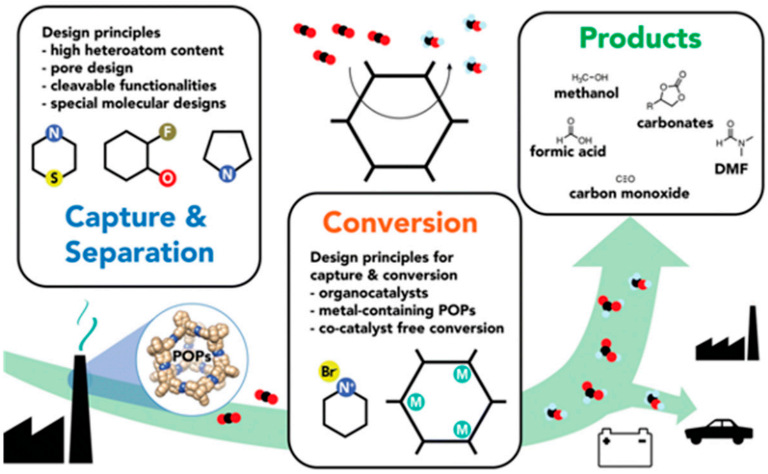

**Figure 11.** Schematic illustration of the design principles of POPs for $CO_2$ capture and separation, and subsequent conversion of $CO_2$. Reproduced with permission from [131] under the CC BY-NC license.

PAFs are high-surface-area materials with tunable chemical functionality, robust structural rigidity, and strong stability, making them highly suitable for applications in gas adsorption and separation, catalysis, and biochemistry. Their extensive benzene ring structures, formed through coupling reactions that create strong carbon–carbon covalent bonds, ensure a stable framework that is resistant to harsh chemical treatments [132]. The schematic illustration of their structure and applications is shown in Figure 12. The specific chemical functionalities of PAFs can be tuned both by the intrinsic properties of the building units and by the pillars formed through coupling reactions [132]. The aromatic groups within PAFs provide physical adsorption sites for $CO_2$ [132,150]. Recent studies have demonstrated that adding polar functional groups, such as dihydrofuran, amine, methoxyl, and hydrogen, to PAFs can enhance their selectivity for $CO_2$ in mixed gases [132,133]. Additionally, the electrostatic interactions between $CO_2$ and PAFs are significant factors influencing $CO_2$ capture performance [132,133,151]. Tian and Zhu conducted an in-depth analysis of the design principles and specific synthesis processes for PAFs in achieving various functions, emphasizing the importance of considering the properties of core building units and different coupling reactions [132].

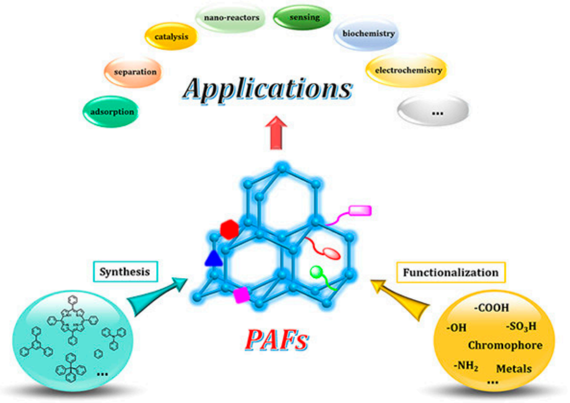

**Figure 12.** Schematic illustration of the structure and applications of PAFs. Reprinted with permission from [132]. Copyright 2020, American Chemical Society.

PIMs share some similarities with other aforementioned porous materials, such as high pore volume, making them suitable for $CO_2$ capture and separation. However, unlike the aforementioned materials, the pores in PIMs result from their contorted molecular structures, which inherently contain micropores due to intra-chain and inter-chain rigidities [135]. These micropores or ultra-micropores enhance the gas permeability of PIMs by fully utilizing the solution diffusion and convective diffusion mechanisms, making them highly efficient for $CO_2$ capture and separation [135,152]. The $CO_2$ adsorption performance of PIMs is affected by factors such as physical aging and plasticization [135]. Therefore, recent research on PIMs has focused on addressing these issues to prevent pore space reduction and decreased capture efficiency during usage. Shamsabadi et al. conducted a detailed evaluation of several newly developed PIMs and their $CO_2$ separation performance, identifying potential PIMs suitable for industrial-scale separation of $CO_2/N_2$ and $CO_2/CH_4$ gas mixtures [135]. Yu et al. designed and synthesized an improved PIM, known as cyclohexyl-fused spirobiindane-based PIM (CCS-PIM), which exhibits a high specific surface area and excellent $CO_2$-selective adsorption capacity [134,153]. The molecular structure of CCS-PIM is shown in Figure 13. This CCS-PIM features a six-membered ring-locking structure within the polymer backbone, resulting in a non-distorted chain structure with well-regulated micropore spaces. The precisely tuned pore size not only contributes to a highly rigid structure but also significantly enhances the molecular sieving effect, leading to outstanding gas separation performance [134].

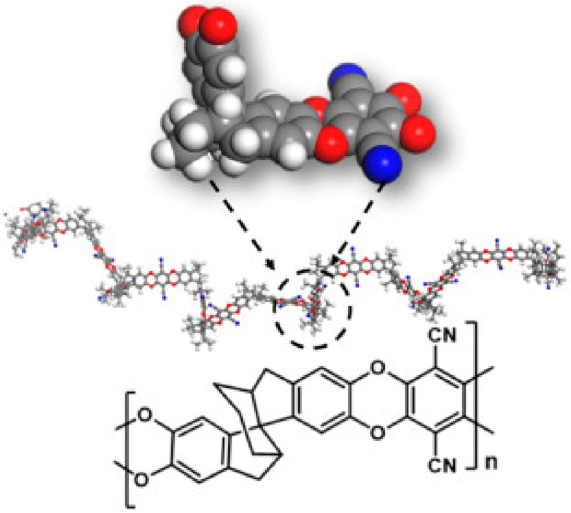

**Figure 13.** Chemical structure of CCS-PIM featuring a non-distorted chain structure with well-regulated micropore spaces for enhanced $CO_2$ separation performance. Reprinted with permission from [134] under the CC BY-NC license.

## 6. Emerging DAC Technologies

In addition to the aforementioned established technologies, to address the growing urgency for more efficient and scalable solutions for DAC, some emerging technologies, including electro-swing adsorption (ESA), moisture-swing adsorption (MSA), and membrane-based separation (m-DAC), have been studied as promising alternatives.

### *6.1. Electro-Swing Adsorption (ESA)*

ESA is a method that separates $CO_2$ from high-concentration sources and the air by altering the charge to achieve capture and release of $CO_2$ [154]. Specifically, $CO_2$ is adsorbed when the solid electrode is negatively charged and released when the electrode is positively charged. The notable advantages of this $CO_2$ separation method include several key aspects. Firstly, it allows for flexible adjustment and efficient operation by enabling the stacking and expansion of electrochemical cells according to the required capacity within a limited space. Secondly, the adsorption and release processes only require charge control, simplifying the operation and reducing the energy consumption associated with the regeneration of liquid solvents and solid sorbents. Additionally, this method simplifies the system's complexity by eliminating the need for additional equipment, thereby reducing maintenance and operational costs in terms of time, labor, and economics. These advantages highlight the significant potential of ESA in carbon capture technology, making it highly efficient and adaptable to various scales and conditions of carbon capture requirements.

To enable ESA for the capture and release of $CO_2$, electrochemical cells or electrode materials are required to facilitate the electrochemical processes [154]. Studies have shown that compounds such as quinones [154,155], 4,4′-bipyridine [154,156], and thiolates [157,158] can serve as carrier molecules for $CO_2$ during the electrochemical processes of adsorption and desorption. Quinones, in particular, exhibit superior electrochemical performance and have the potential to achieve near 100% purity of released $CO_2$ [154], making them the preferred material for $CO_2$ oxidation–reduction activity carriers in electrochemically mediated separation processes [154,155].

Voskian and Hatton designed a faradaic electrochemical cell utilizing quinones for $CO_2$ capture and release [154]. The structure and operational principle of this cell are illustrated in Figure 14. The cell comprises two cathode electrode substrates coated with polyanthraquinone–CNT (PAQ-CNT), a composite material of quinone and carbon nanotubes (Q–CNT), which serves as a mediator for the adsorption and desorption of $CO_2$ molecules via its redox reactions. An anode electrode substrate coated with polyvinylferrocene–CNT (PVFc-CNT), a composite of ferrocene and CNTs (Fc–CNT), is positioned between the two cathode substrates to provide electrons for the quinone's redox reactions. Separator membranes are placed between the cathode and anode substrates to prevent direct electron transfer and allow ion passage. The use of CNT composite materials, with their high surface area and conductivity, facilitates effective ion transfer through the electrolyte during electrode activation and deactivation, allowing for $CO_2$ diffusion during the capture process. During $CO_2$ capture with this cell, a reduction potential is applied to the outer cathode electrode, causing the PAQ-CNT composite to absorb electrons and undergo a reduction reaction, leading to a carboxylation reaction between $CO_2$ and quinone for $CO_2$ capture. Subsequently, when an oxidation potential is applied to the outer cathode electrode, the PAQ-CNT releases electrons and undergoes an oxidation reaction, releasing the adsorbed $CO_2$. The inner PVFc-CNT electrode serves as the electron source and sink for the quinone reduction and oxidation [154]. These electrochemical cells can be stacked to form a contactor with parallel passages in a flow device, thereby providing a larger surface area for contact with $CO_2$ in the feed stream, enhancing the efficiency of $CO_2$ capture in the ESA process [154]. This solid-state faradaic ESA system has demonstrated exceptional performance in $CO_2$ capture. Its compact and flexible architecture allows for stacking to create a suitable contactor with a large surface area for efficient $CO_2$ capture. The system exhibits effective $CO_2$ capture capacity, maintaining up to 10% $CO_2$ even at concentrations as low as 0.6%. It achieves a high faradaic efficiency of over 90% and low energy consumption ranging from 40 to 90 kJ per mole of $CO_2$ captured. Additionally, the electrochemical cells show great durability, with less than 30% capacity loss after 7000 cycles [154]. These promising results underscore the significant potential of this ESA system for industrial applications.

The current status of this technology is in the laboratory-scale testing phase, with ongoing research focusing on enhancing the performance characteristics of the redox materials [159], such as capacity [160], kinetics [159,160], and chemical and physical stability [148]. Simultaneously, relevant cost analyses are being conducted to advance potential large-scale deployment in the future [160].

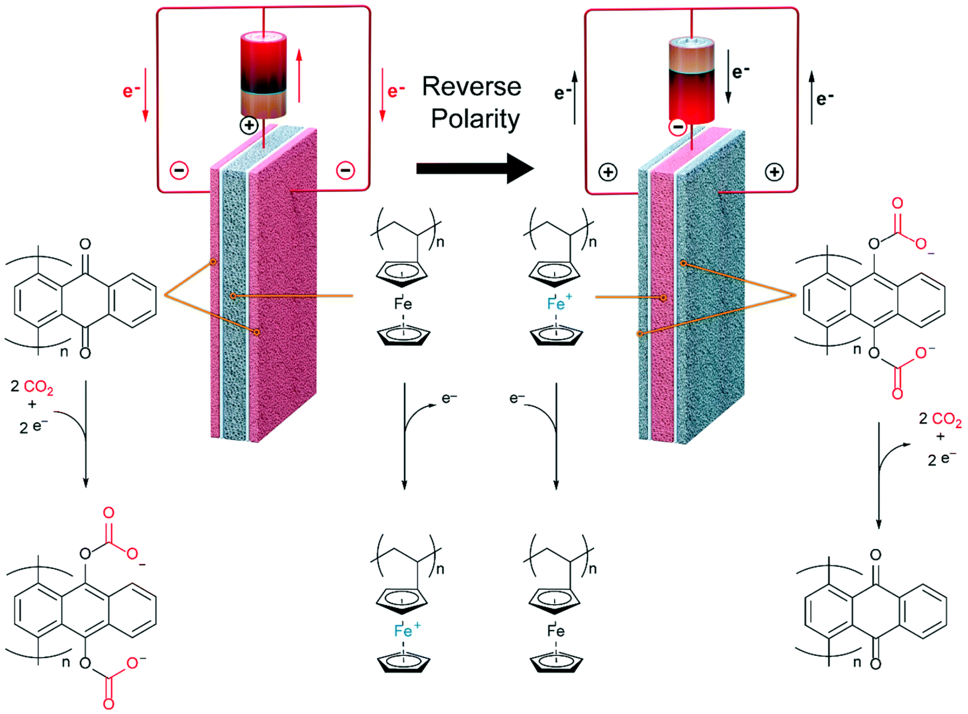

**Figure 14.** Schematic diagram of a single ESA electrochemical cell for $CO_2$ capture and release. Reprinted with permission from [154] under the CC BY-NC license.

### *6.2. Moisture-Swing Adsorption (MSA)*

With its advantage of reduced energy consumption, MSA is considered to be a method capable of replacing the current temperature-swing process in S-DAC [161–163]. Specifically, MSA involves adsorbing $CO_2$ under dry conditions and desorbing it under humid conditions by altering the environmental water vapor pressure at low temperatures (45 °C). Compared to the temperature-swing method used in current S-DAC systems, MSA requires humidity control and lower temperature conditions, making it more operationally convenient while reducing the energy consumption associated with heating. Furthermore, its low temperature requirement facilitates integration with other processes and energy systems, such as utilizing solar energy or waste heat to provide the energy needed for humidification [164].

The fundamental mechanism for $CO_2$ adsorption and desorption in MSA is the change in the free energy of the chemical reaction between carbonate ions and water molecules. Specially, the decrease in the number of water molecules in sorbents leads to a decrease in the free energy change, thereby promoting the capture of $CO_2$ [165]. The adsorbent used in MSA is moisture-sensitive, interacting with water to affect the energy states of carbonate, bicarbonate, and hydroxide ions through hydration and dehydration. As a result, the equilibrium between these ions is altered to achieve $CO_2$ capture and release. The schematic diagram of MSA for $CO_2$ capture and release, along with the potential moisture-driven sorbents, is shown in Figure 15.

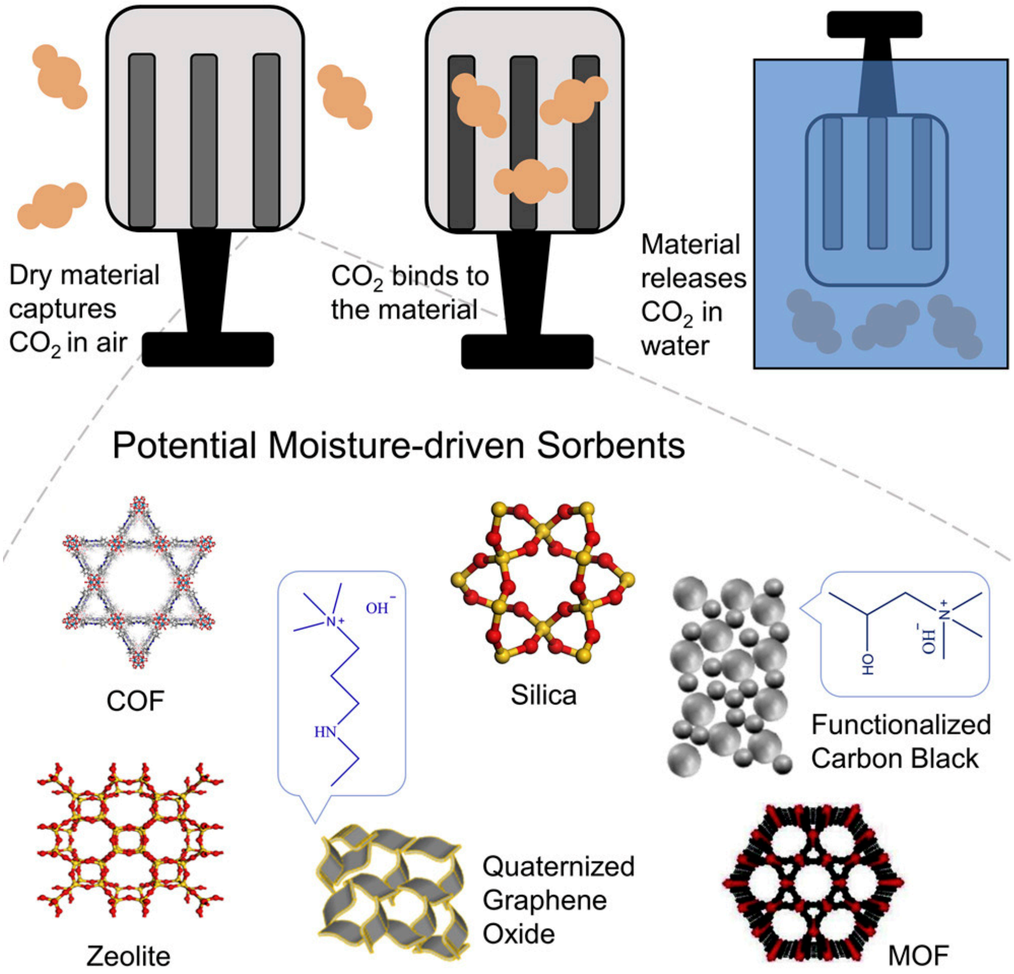

**Figure 15.** Schematic diagram of MSA for $CO_2$ capture and release with potential moisture-driven sorbents. Reprinted with permission from [165]. Copyright 2020, Elsevier.

Recent studies have proven that ion-exchange resins are ideal moisture-driven sorbents in MSA due to their excellent ion-exchange capacity, sensitivity to changes in ambient humidity, and low sorption heat for energy saving [165]. Shi et al. demonstrated through simulation [166] and experimental results [165] that ion-exchange resins can serve as moisture-driven $CO_2$ sorbents by enabling $CO_2$'s capture and release through the manipulation of water activity in the surroundings of the sorbent, leveraging the isolated carbonate ion hydration in these materials. Specifically, low humidity causes the functional groups of the ion-exchange resin to compete with water molecules, leading to water dissociation on the surface and the formation of bicarbonate ions. This process facilitates direct $CO_2$ capture by adsorbing $CO_2$ onto hydroxide ions. Conversely, increasing the humidity results in more water molecules on the sorbent's surface, causing bicarbonate ions to revert to carbonate and release $CO_2$. The authors experimentally demonstrated that quaternary ammonium ions or functional groups provide a fixed positive charge capable of carrying $CO_3^{2-}$ ions. Using polystyrene resin with quaternary ammonium ions, they observed significant changes in $CO_2$ concentration due to its capture and release under varying humidity conditions [165]. Subsequently, based on the properties of quaternary ammonium ions, some studies have focused on further optimizing ion-exchange resins as moisture-driven sorbents [161,167]. Wang et al. proposed an advanced method for improving the properties of ion-exchange resins by grafting quaternary ammonium functional groups onto high-surface-area mesoporous polymers, resulting in a sorbent with ultra-high kinetics [167]. This method effectively utilizes the uniform cylindrical pore structure to efficiently attach quaternary ammonium functional groups to active substitution sites. This optimized structure not only enhances the efficiency of the functional groups but also leverages the capillary action of the pore structure [167–171], further enhancing the $CO_2$ capture capacity. Building on the properties of quaternary ammonium ions, Biery et al. further optimized the mechanical performance of sorbents containing quaternary ammonium ions. Specifically, they designed and synthesized sulfone-based multiblock copolymers containing ammonium functionalities [161]. This synthesis leverages the combined properties of polysulfones, which offer excellent strength and thermal stability, and quaternary ammonium polymers, which provide superior ion-exchange properties. A series of multiblock copolymers containing both polydiallyldimethylammonium (PDADMA) and polysulfone (PSf) blocks were synthesized, where the PDADMA blocks directly capture $CO_2$ and the PSf blocks provide mechanical integrity. These optimizations of moisture-driven sorbents enhance the capture efficiency and durability during application, promoting the broader practical use of moisture-driven DAC.

### *6.3. Membrane-Based Separation (m-DAC)*

Applying membrane separation technology to DAC is known as m-DAC [33]. The core principle of membrane separation technology lies in utilizing specific permeable membranes to control the transfer of substances across the membrane, thus achieving the separation and capture of target substances. Therefore, using membranes with high $CO_2$ permeability, m-DAC allows $CO_2$ to pass through while retaining other gases on the opposite side, effectively separating $CO_2$ from the air.

When compared to other DAC technologies, m-DAC stands out for its low energy consumption, making it a potentially viable energy-saving solution [40]. Additionally, it offers straightforward and stable operation, along with a small footprint [32]. However, a current challenge limiting the widespread adoption of this technology is the low flux associated with membrane separation due to the low partial pressure of $CO_2$ in air [172,173], resulting in poor economic viability. Addressing this challenge, recent efforts in optimizing m-DAC technology have primarily focused on the development of membrane materials with high $CO_2$ permeability and selectivity. Significant progress has been achieved in advancing membrane materials.

Thin-film composite or ultrathin-film composite (TFC) membranes, characterized by nanometer-scale thicknesses, are recognized ideal for m-DAC [174]. The structural composition of TFC membranes is depicted in Figure 16, comprising a selective layer, a gutter layer (alternatively referred to as the intermediate layer), and a porous support. Building on the fundamental principle that the ethylene oxide (EO) unit facilitates favorable interactions with $CO_2$ over light gases for separation [175], Fu et al. proposed a class of TFC membranes containing high-molecular-weight amorphous polyethylene oxide (PEO) with high EO moieties to enhance $CO_2$ permeability and flux [172]. Specifically, this optimized membrane system comprises a polymer membrane matrix with a selective layer containing PEO and a gutter layer composed of polydimethylsiloxane (PDMS). The incorporation of multiple PEO blocks interspaced with a specially designed terephthalic spacer into the base polymer membrane matrix significantly enhances the $CO_2$ separation ability without inducing crystallinity [172]. Meanwhile, the PDMS gutter layer serves as a protective coating to maintain membrane surface smoothness and efficiency by preventing penetration of the diluted polymer solution into the porous structure, ensuring smooth gas separation [172,176]. Moreover, researchers have sought to enhance gas permeance by reducing membrane thickness, given the general inverse relationship between gas flux and membrane thickness. Yoo et al. proposed using the Teflon-based material AF2400 instead of PDMS as the gutter layer, with a thickness of only 75 nm, coupled with a 70 nm selective layer, forming an ultrathin membrane [174]. This optimization reduces membrane thickness and significantly enhances $CO_2$ permeance sixfold compared to membranes with PDMS as the gutter layer, thus greatly improving the $CO_2$ separation efficiency. To further reduce membrane thickness, Fujikawa et al. proposed utilizing the inherent gas permeance property of PDMS due to its dynamic polymer chain nature, enabling the direct production of free-standing PDMS nanomembranes for $CO_2$ separation [177]. By controlling the spinning speed and PDMS concentration during the spin-coating process, they achieved a thickness of 34 nm. The experimental results demonstrated a fourfold increase in $CO_2$ permeance from 10,000 GPU to 40,000 GPU when reducing the PDMS membrane thickness from over 100 nm to 34 nm. These optimizations result in TFC membranes with higher $CO_2$ permeance and selectivity, reducing the gas permeance resistance and making $CO_2$ gas capture from diluted emission sources more feasible.

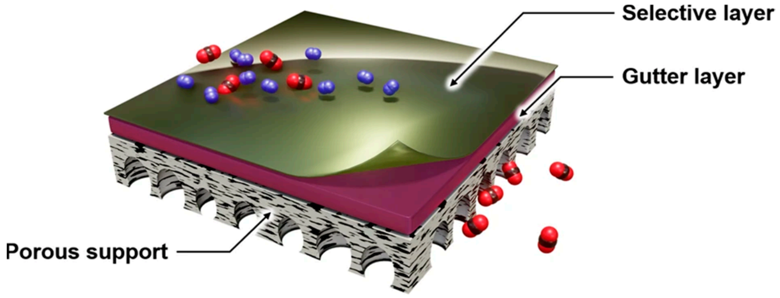

**Figure 16.** Schematic illustration of a thin-film composite membrane for m-DAC. Reprinted with permission from [33] under the CC BY license.

Mixed-matrix membranes (MMMs) are another promising candidate for m-DAC. These membranes incorporate various porous fillers, such as carbon molecular sieves [178], zeolites [179,180], MOFs [181], and COFs [182,183], into a polymer matrix to enhance $CO_2$ separation and enable repeated use. MMMs combine the high adsorption capacity of porous fillers with the mechanical strength of polymers. Typically, MMMs can be fabricated using techniques similar to conventional polymeric membranes [184,185], with fillers ranging from spherical with a low aspect ratio to thin platelet-type with a very high aspect ratio [186]. Research on MOF-based and COF-based MMMs has been increasing due to their advantages as porous materials with tunable pore sizes and properties [181–183,185].

MOF-based MMMs improve $CO_2$ separation efficiency by altering the microenvironment of the MOF and polymer matrix [187], enhancing their adhesion [188], and rationally designing them for desired interfacial properties [188]. Additionally, research suggests that the mechanical properties of MOF-based MMMs, including thermomechanical, stress–strain, and viscoelastic properties, can be enhanced through interactions between the MOF and the polymer matrix [189,190]. COF-based MMMs show potential for m-DAC due to the thermal and chemical stability of covalently bonded COFs as ideal fillers. While direct use of pristine COFs as fillers in MMMs is feasible [191,192], studies have shown that modifying COFs before use can further improve $CO_2$ separation performance [193,194]. Liu et al. proposed a multi-function integration strategy to enhance COF-based MMMs' $CO_2$ separation performance [194]. They optimized the COF fillers' properties by considering their entire morphological structure, aperture adjustment, and channel decoration. The inner and outer surfaces of the improved COF fillers were then modified with polyethylene glycol monomethyl ether (PEG) to form hollow microspheres, reducing the mass transport resistance. Finally, these modified COF fillers were incorporated into a commercial Pebax polymer matrix to create the designed COF-based MMM for $CO_2$ capture. This COF-based MMM utilizes PEG functionalization to modify the COF inter-surface by providing ethylene oxide groups, which have an affinity for quadrupolar $CO_2$ and decrease the pore size to enhance $CO_2$'s solubility selectivity and diffusion selectivity. Meanwhile, PEG chains on COFs' outer surface improve compatibility between the COF fillers and the Pebax matrix. As a result, this COF-based MMM achieves superior $CO_2$ separation performance.

It is noteworthy that the evaluation of different membranes for m-DAC can be effectively conducted using advanced simulation software and computational modeling tools [195]. Platforms such as ASPEN HYSYS [196], Aspen Plus V11 flowsheeting software [33], and COMSOL Multiphysics [195] are invaluable for predicting and optimizing the performance of various membrane materials, providing a cost-efficient means to assess and enhance their performance.

## 7. Comparison of DAC Technologies

In the preceding sections, L-DAC, S-DAC, and emerging DAC technologies have been comprehensively introduced. The principles, commonly employed materials, advantages, and disadvantages of these technologies are summarized in Table 3 for a more intuitive comparison.

**Table 3.** Comparison of different DAC technologies.

| Technology | | Principle | Commonly Employed Material | Advantage | Disadvantage |
|---|---|---|---|---|---|
| L-DAC | | The liquid solvent reacts with $CO_2$ to form carbonates for capture, and it releases $CO_2$ upon heating | Alkaline solutions | Large-scale operation;<br>Continuous operation at steady state without interruption;<br>Low-cost raw materials with good selectivity and capture capacity | High temperature requirement;<br>High energy consumption;<br>Requirement for corrosion-resistant equipment |
| S-DAC | | The solid sorbent captures $CO_2$ from ambient air at room temperature and atmospheric pressure, and then releases $CO_2$ under low pressure and moderate temperatures through a temperature-vacuum swing process | Amine-based sorbents | Modular and scalable operations;<br>Lower energy consumption than L-DAC | Batch operations causing complex plant structures;<br>Special construction required for cycling temperature and pressure conditions;<br>High construction costs;<br>Sorbents with low sustainability |
| Emerging DAC technologies | ESA | The electrochemical cell utilizes charge modulation to control the adsorption and desorption processes, capturing $CO_2$ when negatively charged and releasing it when positively charged | Electrochemical cell;<br>Electrode materials | Space-efficient structure;<br>Convenient operation with no additional equipment required;<br>Low energy consumption;<br>Effective capture capacity;<br>Good durability | High investment costs |
| | MSA | The moisture-sensitive sorbents rely on chemical reactions between carbonate ions and water molecules to alter energy states, facilitating $CO_2$ capture in dry conditions and $CO_2$ release in wet conditions | Ion-exchange resins | Low energy consumption;<br>Convenient integration with low-carbon energies | Consumption of a large amount of water;<br>Sensitive to practical weather conditions |
| | m-DAC | The membrane utilizes selective permeability properties to enable the separation and capture of $CO_2$ from air | Ultrathin-film composite (TFC) membrane;<br>Mixed-matrix membranes (MMMs) | Low energy consumption;<br>Low carbon footprint | Low throughput;<br>High material costs |

L-DAC and S-DAC, as extensively industrialized technologies, are notable for their technical maturity. However, their drawbacks cannot be overlooked. L-DAC suffers from high energy consumption and requires corrosion-resistant equipment. S-DAC's challenges include complex plant structures due to batch operations and specialized construction for cycling temperature and pressure conditions, resulting in high investment costs. These significant drawbacks may limit their broader global adoption.

Emerging DAC technologies, including ESA, MSA, and m-DAC, show considerable promise, albeit they are still in the research and development phase, with limited large-scale applications. These technologies boast significant advantages, particularly in their low energy consumption for $CO_2$ capture and separation. Their operational simplicity positions them as highly viable for future DAC applications. Notably, innovative polymer materials used as moisture-sensitive sorbents in MSA technology, along with their synthesis routes, have been submitted for patent applications [197,198]. The Mechanical Trees$^{TM}$ based on MSA technology utilizing these sorbents are currently undergoing commercialization through a collaboration between Arizona State University and Carbon Collect.

## 8. Practical Applications of DAC

The application status of DAC technology serves to inform global industries about its practical implementation. According to the IEA, as of 2023, there are 27 operational DAC plants globally, mainly situated in North America, Europe, Japan, and the Middle East. These facilities collectively capture nearly 0.01 Mt $CO_2$ annually. Furthermore, plans are underway for the development of at least 130 additional DAC facilities, at various stages of implementation [199]. Globally, the leading companies focused on DAC include North American companies such as Carbon Engineering, Global Thermostat, CarbonCapture, and Baker Hughes. European companies in this field include Climeworks, Antecy, Skytree, Carbon Collect, and Hydrocell [30].

Currently, North America hosts several notable DAC plants, exemplifying the region's engagement with DAC technology [26]. The basic information of typical representative DAC facilities in North America is shown in Table 4.

Notably, the United States stands out for its robust policy support. With the introduction of the Inflation Reduction Act (IRA) in 2022, the 45Q tax credit for $CO_2$ capture was increased to USD 180 per ton stored. This policy support, coupled with a capture threshold as low as 1000 tons of $CO_2$ annually, positions the United States as a global leader in DAC applications. The current notable projects under development in the United States include STRATOS in Texas, the Oxy-CE Kleberg County project, the HIF eFuels Matagorda County project, the Bison project, and the Adams County project [199].

In the United States, DAC plants widely adopt the mature and well-developed L-DAC technology using alkaline solutions, as discussed in Section 4. This technology, developed and improved by Carbon Engineering (CE), a Canadian-based clean energy company, utilizes KOH solution as the liquid solvent. It features a contactor with a cross-flow pattern for air and the alkaline solution, ensuring efficient contact for the reaction. Aspen Plus simulation is employed to determine the operational parameters related to energy and material balances [41]. Typical industrial-scale applications of this technology include the STRAROS DAC1 and the Oxy-CE Kleberg County project, both located in Texas, USA. The STRAROS DAC1, which employs CE's L-DAC technology, was constructed by Oxy Low Carbon Ventures (OLCV) through its subsidiary 1PointFive (Houston, TX, USA). This facility, using a scalable setup, aims to capture 1.0 Mt $CO_2$/year and, ultimately, sends compressed pure $CO_2$ to geological storage sites for permanent sequestration. Expected to commence operation in 2024, it is currently the world's largest DAC facility [199,200]. The Oxy-CE Kleberg County project, the second DAC facility site in the United States, employs the same design as STRAROS DAC1, with CE's L-DAC technology [201]. Located in the Gulf Coast region, the DAC plant leverages ideal porous formations for geological storage, ensuring safe and verifiable $CO_2$ removal and storage. The project adopts an innovative deployment approach to standardize factory design, accelerate construction, and establish a supplier supply chain for local partners, facilitating rapid progress.

**Table 4.** Representative DAC facilities in North America.

| Project | Location | Operating Company | Capture Capacity | Capture Technology | Types of Utilization and Storage | References |
|---|---|---|---|---|---|---|
| STRAROS DAC1 | Texas Permian Basin | 1 PointFive (a subsidiary of Occidental) and Carbon Engineering | 1.0 Mt $CO_2$/year | L-DAC | Geological storage | [200] |
| Oxy-CE Kleberg County project | Gulf Coast region, Texas, US | 1 PointFive (a subsidiary of Occidental) and Carbon Engineering | 30 Mt $CO_2$/year | L-DAC | Geological storage | [201] |
| HIF eFuels Matogorda County project | Matagorda County, Texas, US | Highly Innovative Fuels (HIF) and Baker Hughes | 25 Mt $CO_2$/year | MOFs as primary sorbents | eFuel production | [202] |
| Project Basin | Wyoming, US | CarbonCapture and Frontier Carbon Solutions | 5-Megaton-scale | S-DAC as the primary method, possibly combined with MOFs and hybrid solutions | Deep saline aquifer storage | [199,203] |
| Adams County project | Colorado, US | Global Thermostat | 1000 tonnes $CO_2$/year | S-DAC | Valuable products | [199,204] |
| DAC R&D facility | Squamish, British Columbia, Canada | Carbon Engineering | 1 Mt $CO_2$/year | L-DAC | Fuel production | [41] |

The HIF eFuels Matagorda County project, a collaboration between Baker Hughes (BKR) (Houston, TX, USA) and HIF Globa (Houston, TX, USA), involves testing Baker Hughes's Mosaic DAC technology pilot units in Matagorda County, Texas. This technology utilizes MOFs as the primary sorbent material and aims to accelerate DAC's deployment at a commercial scale [202]. By leveraging the porous structure and adsorption capabilities of MOFs, the project implements a groundbreaking low-cost DAC initiative to accelerate $CO_2$ capture. The captured $CO_2$ is then combined with green hydrogen to produce 150,000 barrels of eFuels per day, contributing to the decarbonization of over 5 million vehicles in use.

Project Basin in Wyoming utilizes a low-cost modular DAC system developed by CarbonCapture Inc. (Los Angeles, CA, USA) to filter $CO_2$ from the air [199]. The technology allows for scalability and integration with extensive renewable energy facilities like wind and solar power. Subsequently, Frontier Carbon Solutions (Dallas, TX, USA) collects this captured $CO_2$ and injects it into deep saline aquifers using Class VI injection wells managed by the Wyoming Department of Environmental Quality, as per EPA regulations [203]. The Adams County project by Global Thermostat (Denver, CO, USA) features one of the world's largest DAC machines. This project has been capturing over 1000 tonnes of $CO_2$ annually since late 2022, using S-DAC [203].

Furthermore, the Carbon Engineering Innovation Center, situated in Squamish, British Columbia, Canada, stands as the world's largest facility dedicated to research and development in DAC, established by CE since 2015 [41]. It serves as an advanced research platform where CE's DAC technologies undergo testing before implementation in practical applications, including the aforementioned STRAROS DAC1 and Oxy-CE Kleberg County project.

In Europe, several countries have established DAC plants, including Switzerland, Iceland, the United Kingdom, Norway, Italy, Germany, and the Netherlands. Among these, Germany and the Netherlands host DAC plants of modest scale, capturing below 50 t $CO_2$/year. DAC plants with larger $CO_2$ capture capacities are predominantly found in the United Kingdom, Norway, and Iceland. The basic information of these typical DAC plants is detailed in Table 5.

**Table 5.** Representative DAC facilities in Europe.

| Project | Location | Operating Company | Capture Capacity | Capture Technology | Types of Utilization and Storage | References |
|---|---|---|---|---|---|---|
| North-East Scotland DAC Project | United Kingdom | Storegga and Carbon Engineering | 500,000 to 1,000,000 tonnes of $CO_2$/year | L-DAC | Geological storage | [205] |
| Kollsnes DAC project | Norway | Carbon Removal, Carbon Engineering, and Oxy Low Carbon Ventures | 500,000 to 1,000,000 tonnes of $CO_2$/year | L-DAC | Offshore geological storage | [206] |
| Capricorn | Hinwil, Switzerland | Climeworks | Several hundred tons of $CO_2$/year | S-DAC | Vegetable fertilization and beverage industry | [207] |
| Arctic Fox | Hellishidi, Iceland | Climeworks | 50 tons of $CO_2$/year | S-DAC | Geological stroage | [208] |
| Orca | Hellisheidi, Iceland | Climeworks | 4000 tons of $CO_2$/year | S-DAC | Geological storage | [209] |
| Mammoth | Hellisheidi, Iceland | Climeworks and Carbfix | 36,000 tons of $CO_2$/year | S-DAC | Geological storage | [210] |

The DAC facility located in the northeastern part of Scotland, UK, is a collaborative effort between Storegga, a UK-based company, and Carbon Engineering. Expected to start operations in 2026, this DAC plant will mark Europe's inaugural large-scale DAC facility, integrating DAC technology with geological storage, with support from Scotland's renewable energy and oil and gas industry expertise. It is expected to permanently remove between 500,000 and 1,000,000 tonnes of $CO_2$ annually [205].

The Kollsnes DAC project, located in Norway, is a collaborative effort involving three companies: Carbon Removal, Carbon Engineering, and Oxy Low Carbon Ventures [206]. This DAC project utilizes L-DAC technology and is expected to capture between 500,000 and 1,000,000 tonnes of $CO_2$ from the atmosphere annually. Leveraging policy support from the Norwegian government and mature technologies from the reliable renewable energy, oil, and natural gas industries, significant amounts of $CO_2$ will be permanently stored in subsea geological storage sites through this project.

The DAC plants in Switzerland and Iceland primarily employ S-DAC technology with filters containing solid sorbent materials, as described in Section 5. This technology is designed and developed by Climeworks, a Swiss company specializing in direct air capture and storage (DAC+S). These S-DAC facilities exclusively use renewable energy, waste-to-energy, or other waste heat sources, significantly minimizing their carbon footprint and enhancing the sustainability and efficiency of their energy usage. Typical DAC plants employing S-DAC technology include the Capricorn plant in Switzerland and the Artic Fox, Orca, and Mammoth plants in Iceland. The Capricorn project, situated near the town of Hinwil, Switzerland, started operations in 2017, marking Climeworks' first industrial-scale DAC plant [207]. It consists of 18 $CO_2$ collectors and utilizes waste heat from a local waste incineration plant to power the capture process. This facility is capable of capturing hundreds of tons of $CO_2$ annually. A portion of the $CO_2$ captured from the air is delivered to nearby greenhouses for vegetable fertilization, while another portion, after liquefaction, is transported to the beverage industry for utilization.

The three DAC projects in Iceland are all based in Hellisheidi, using renewable energy such as geothermal energy from local geothermal power plants to power the DAC plants. Among these projects, Arctic Fox, which launched in 2017, is the first DAC facility built by Climeworks in Iceland [208]. One $CO_2$ collector was established in this project, with the ability to capture 50 tons of $CO_2$ annually. The captured $CO_2$ is mixed with water using Carbfix's technology and then pumped deep underground, where a natural mineralization reaction occurs between $CO_2$ and basalt rocks, achieving permanent geological storage of $CO_2$. After the successful operation of this project, Climeworks established another DAC plant named Orca in 2021 [209]. This project adopts an improved design and uses eight collectors, each with a collection capacity of 500 tons. The entire plant can capture up to 4000 tons of $CO_2$ per year, making it the largest direct air capture and storage plant in the world. Starting in 2022, Climeworks began the construction of a DAC plant called "Mammoth", which is expected to be completed and put into use in 2024 [210]. It is expected that, after the plant is put into use, it will be able to capture up to 36,000 tons of $CO_2$ per year, which will constitute an important milestone in increasing the carbon removal capacity from thousands to tens of thousands of tons per year.

Despite the current global application of DAC technology being primarily small-scale, increasing emphasis on $CO_2$ emissions worldwide is leading to greater funding for DAC research and implementation, which will accelerate its large-scale deployment. In 2021, the United States allocated USD 3.5 billion for DAC hubs and launched a DAC Prize program with USD 115 million for commercial and pre-commercial projects [26]. Similarly, new R&D funding in countries such as Australia, Canada, Japan, and the UK underscores the international recognition of the importance of developing and scaling up DAC technologies [26]. Additionally, regions with high renewable energy potential, including the Middle East, China, Europe, North Africa, and the United States, have been identified as some of the least-cost locations for DAC deployment [26]. The abundance of renewable energy in these regions will significantly reduce DAC costs, making them ideal for the large-scale implementation of DAC in the future.

## 9. Challenges and Future Directions

Compared to point sources of high-concentration $CO_2$, such as refineries, power plants, or cement factories, the inherent dilution of $CO_2$ in the atmosphere results in significantly lower concentrations. This characteristic necessitates denser deployment, larger operational scales, increased energy supply, and more effective but higher-cost materials for DAC facilities. Consequently, the cost of DAC significantly exceeds that of traditional capture techniques when capturing the same amount of $CO_2$. Thus, the economic feasibility of DAC faces significant challenges, which are pivotal factors limiting its widespread application. To address these challenges, efforts can be directed towards optimizing energy supply, refining technologies and process designs, and strengthening financial support and incentive measures from governments and international organizations.

Currently, DAC plants primarily rely on natural gas as their primary energy source, with some utilizing waste heat from nearby incineration plants and geothermal energy. Transitioning towards greater utilization of low-cost renewable energy sources instead of natural gas could markedly decrease operational expenses for DAC facilities. Renewable sources like wind, solar (or photovoltaic), and geothermal energy stand out as particularly promising alternatives. Fasihi et al. conducted techno-economic analyses of DAC technologies and demonstrated that DAC plants powered by hybrid PV–wind–battery energy systems could position DAC facilities to compete on cost with traditional carbon capture methods used in $CO_2$ point sources [163]. Further in-depth research focusing on cost analysis of low-carbon energy sources such as geothermal energy, solar power, nuclear power, electricity supply, and waste heat for DAC holds the promise of significantly reducing operational costs and promoting wider adoption of DAC plants.

In the advancement of technology and processes, experimental studies and on-site testing of DAC plants in different environments are crucial for the global application of DAC technology. One significant advantage of DAC technology lies in its flexibility in site selection, which should be fully utilized to achieve global net-zero carbon emissions. Based on the current operational status of DAC facilities worldwide, DAC plants can operate successfully in diverse environmental conditions, even in harsh environments like Iceland. However, some uncertainties still persist, particularly in extremely dry or humid climates, or in areas with severe air pollution, where the feasibility of DAC facilities' operation remains undetermined. Extremely dry climatic conditions may further reduce the concentration of $CO_2$ in the air, while humid conditions could affect the performance and durability of DAC equipment. Additionally, polluted air may contain other chemical substances that could interfere with or damage DAC facilities. To address these issues, future research can begin by using simulation software and conducting small-scale laboratory experiments under simulated environmental conditions to optimize airflow and relevant parameters after air enters the equipment. Subsequently, small-scale testing should be conducted in real environments, equipped with necessary monitoring devices to collect operational data and validate the laboratory findings. For highly polluted conditions, effective air filtration and pretreatment technologies could be integrated into DAC facilities to remove harmful substances that may affect DAC equipment's performance, ensuring smooth $CO_2$ capture operations.

The continuous investment in research and development and comprehensive policy support are crucial for the advancement of DAC technology. Sufficient government funding and investment, along with effective market mechanisms like an improved carbon trading market system, tax incentives, and subsides, as well as strong policy support, can incentivize relevant researchers and companies to actively improve process workflows, optimize equipment designs, reduce raw material costs, and conduct more on-site testing. Furthermore, given the global impact of climate change, international cooperation and coordination are particularly important. The sharing of technology and expertise facilitates the more effective and rapid deployment of DAC plants worldwide.

Furthermore, broader utilization of $CO_2$ can significantly contribute to creating an ideal market and reducing costs for DAC. One important and typical application involves using $CO_2$ captured by DAC technology for synthetic fuel production. Current research has achieved the synthesis of fuels by reacting $CO_2$ captured by DAC with hydrogen [28,211,212]. In such studies, renewable energy sources such as wind and solar power are utilized to provide heat or electricity for electrolysis, facilitating sustainable hydrogen generation to react with $CO_2$ for synthetic fuel production. Through this approach, various fuels, including methane, methanol, and diesel, can be produced [213]. These synthetic fuels find notable application prospects in the transportation sector, particularly in aviation, offering a viable solution for reducing emissions from conventional fossil fuels [26]. However, compared to fossil fuels, the current cost of synthesizing such fuels remains relatively high. Therefore, future research efforts will focus on reducing the synthesis costs of these fuels. Additionally, integrating appropriate electrochemical conversion processes to react $CO_2$ captured by DAC with other raw materials to produce engineering polymers/resin precursors, specialty chemicals, and bulk chemicals will be a promising future research direction [2].

Additionally, it is worth noting that artificial intelligence (AI) methodologies have gained considerable attention in recent years for their ability to efficiently process and analyze complex data patterns and optimize system operations in CCUS and DAC [214,215]. AI, including related machine learning (ML) methods, has been studied and used for modeling, simulation, and optimization in carbon capture to accelerate the optimization of material selection and expedite the design of capture/utilization systems [216,217]. Future development of more accurate predictive models and optimization algorithms will further promote the broader application of AI technology in the CCUS and DAC fields, with its capacity for rapid analysis of large amounts of real-time data, resulting in higher carbon capture efficiency and lower costs.

## 10. Conclusions

DAC technology, with its capacity to directly capture low-concentration $CO_2$ from the atmosphere without requiring connection to specific emission sources, presents a versatile and scalable solution for mitigating atmospheric $CO_2$ emissions. It is recognized as a pivotal technology in attaining net-zero or negative emissions targets, thereby positioning DAC as a promising pathway for global carbon reduction initiatives and enabling broader carbon neutrality objectives worldwide.

L-DAC and S-DAC, as mature technologies, have been implemented on an industrial scale. Recent advancements in L-DAC have predominantly concentrated on enhancing engineering aspects in practical applications to ensure projects' economic feasibility. This involves optimizing engineering costs while maximizing capture efficiency. Additionally, significant recent research progress has been achieved in exploring alternative solvents for L-DAC, beyond alkaline solutions. Progress in S-DAC has focused on enhancing the performance of amine-based sorbents and assessing porous materials with microscale-to-macroscale pores or voids as potential sorbents for industrial applications.

ESA, MSA, and m-DAC are emerging DAC technologies aimed at providing more efficient and scalable solutions for DAC. Although these new technologies are still in the research and development phase and have not yet been widely implemented, they possess several obvious advantages, such as lower energy consumption, simpler operation, and reduced maintenance and operational costs. These benefits will facilitate their broader application in the future, enabling more efficient atmospheric $CO_2$ capture.

Currently, industrial-scale DAC plants operating in North America and Europe are performing well. The primary constraint on the broader deployment of DAC technology is its economic feasibility. Promoting DAC on a global scale can be achieved by optimizing energy supply, refining technologies and process designs, and strengthening financial support and incentives from governments and international organizations. Additionally, expanding the utilization of $CO_2$, such as using $CO_2$ captured by DAC for synthetic fuel production and the synthesis of other valuable chemical materials, will also help advance the adoption of DAC technology worldwide.

**Author Contributions:** G.L.: original draft writing, resources, and visualization; J.Y.: conceptualization, original draft writing, review, and editing. All authors have read and agreed to the published version of the manuscript.

**Funding:** This research received no external funding.

**Institutional Review Board Statement:** Not applicable.

**Informed Consent Statement:** Not applicable.

**Data Availability Statement:** Not applicable.

**Acknowledgments:** The authors are grateful to the Departments of Chemical Engineering and Petroleum Engineering at the University of Wyoming for their support.

**Conflicts of Interest:** The authors declare no competing interests.

## References

1. Baker, H.S.; Millar, R.J.; Karoly, D.J.; Beyerle, U.; Guillod, B.P.; Mitchell, D.; Shiogama, H.; Sparrow, S.; Woollings, T.; Allen, M.R. Higher $CO_2$ Concentrations Increase Extreme Event Risk in a 1.5 °C World. *Nat. Clim. Change* **2018**, *8*, 604–608. [CrossRef]
2. Yao, J.; Han, H.; Yang, Y.; Song, Y.; Li, G. A Review of Recent Progress of Carbon Capture, Utilization, and Storage (CCUS) in China. *Appl. Sci.* **2023**, *13*, 1169. [CrossRef]
3. Storrs, K.; Lyhne, I.; Drustrup, R. A Comprehensive Framework for Feasibility of CCUS Deployment: A Meta-Review of Literature on Factors Impacting CCUS Deployment. *Int. J. Greenh. Gas Control* **2023**, *125*, 103878. [CrossRef]
4. Han, J.; Li, J.; Tang, X.; Wang, L.; Yang, X.; Ge, Z.; Yuan, F. Coal-Fired Power Plant CCUS Project Comprehensive Benefit Evaluation and Forecasting Model Study. *J. Clean. Prod.* **2023**, *385*, 135657. [CrossRef]
5. Ritchie, H. Sector by Sector: Where Do Global Greenhouse Gas Emissions Come From? OurWorldInData.org. Available online: https://ourworldindata.org/ghg-emissions-by-sector (accessed on 18 September 2020).
6. Bai, X.; Yan, G.; Kong, S.; Yao, J.; Wen, P.; Li, G.; Li, J.; Zhang, J. Suppression of Anthracite Dust by a Composite of Oppositely-Charged Ionic Surfactants with Ultra-High Surface Activity: Theoretical Calculation and Experiments. *Fuel* **2023**, *344*, 128075. [CrossRef]
7. Bai, X.; Yan, G.; Kong, S.; Yang, T.; Yao, J.; Wen, P.; Li, G. Study on the Mechanism of the Influence of Surfactant Alkyl Chain Length on the Wettability of Anthracite Dust Based on EDLVO Theory and Inverse Gas Chromatography. *Fuel* **2023**, *353*, 129187. [CrossRef]
8. Yao, J.; Li, G.; Wu, J. Application of In-Situ Combustion for Heavy Oil Production in China: A Review. *J. Oil Gas Petrochem. Sci.* **2018**, *1*, 69–72. [CrossRef]
9. Yao, J.; Song, Y. Dynamic Analysis Approach to Evaluate In-Situ Combustion Performance for Heavy Oil Production. *J. Oil Gas Petrochem. Sci.* **2019**, *2*, 42–47. [CrossRef]
10. Ivanova, S.; Vesnina, A.; Fotina, N.; Prosekov, A. An Overview of Carbon Footprint of Coal Mining to Curtail Greenhouse Gas Emissions. *Sustainability* **2022**, *14*, 15135. [CrossRef]
11. Yang, B.; Bai, Z.; Zhang, J. Environmental Impact of Mining-Associated Carbon Emissions and Analysis of Cleaner Production Strategies in China. *Environ. Sci. Pollut. Res.* **2021**, *28*, 13649–13659. [CrossRef]
12. Marron, D.B.; Toder, E.J. Tax Policy Issues in Designing a Carbon Tax. *Am. Econ. Rev.* **2014**, *104*, 563–568. [CrossRef]
13. Norouzi, M.; Haddad, A.N.; Jiménez, L.; Hoseinzadeh, S.; Boer, D. Carbon Footprint of Low-Energy Buildings in the United Kingdom: Effects of Mitigating Technological Pathways and Decarbonization Strategies. *Sci. Total Environ.* **2023**, *882*, 163490. [CrossRef] [PubMed]
14. Silaev, V.I.; Klyuev, R.V.; Eremeev, D.V.; Martynova, T.A.; Danilchenko, Y.V. Analysis of the carbon footprint created by mining enterprises. *MIAB Min. Inf. Anal. Bull.* **2023**, *11*, 265–277. [CrossRef]
15. Hickmann, T.; Widerberg, O.; Lederer, M.; Pattberg, P. The United Nations Framework Convention on Climate Change Secretariat as an Orchestrator in Global Climate Policymaking. *Int. Rev. Adm. Sci.* **2021**, *87*, 21–38. [CrossRef]
16. Falkner, R. The Paris Agreement and the New Logic of International Climate Politics. *Int. Aff.* **2016**, *92*, 1107–1125. [CrossRef]
17. Khan, J.; Arsalan, M.H. Solar Power Technologies for Sustainable Electricity Generation—A Review. *Renew. Sustain. Energy Rev.* **2016**, *55*, 414–425. [CrossRef]
18. Hosseini, S.E.; Wahid, M.A. Hydrogen from Solar Energy, a Clean Energy Carrier from a Sustainable Source of Energy. *Int. J. Energy Res.* **2020**, *44*, 4110–4131. [CrossRef]
19. Maka, A.O.M.; Alabid, J.M. Solar Energy Technology and Its Roles in Sustainable Development. *Clean Energy* **2022**, *6*, 476–483. [CrossRef]
20. Li, G.; Yao, J.; Song, Y.; Tang, J.; Han, H.; Cui, X. A Review of the Metallogenic Mechanisms of Sandstone-Type Uranium Deposits in Hydrocarbon-Bearing Basins in China. *Eng* **2023**, *4*, 1723–1741. [CrossRef]
21. Li, G.; Yao, J. A Review of In Situ Leaching (ISL) for Uranium Mining. *Mining* **2024**, *4*, 120–148. [CrossRef]
22. Tavner, P. Wind Power as a Clean-Energy Contributor. *Energy Policy* **2008**, *36*, 4397–4400. [CrossRef]
23. Kaygusuz, K. Wind Power for a Clean and Sustainable Energy Future. *Energy Sources Part B Econ. Plan Policy* **2009**, *4*, 122–133. [CrossRef]
24. Mon, M.T.; Tansuchat, R.; Yamaka, W. CCUS Technology and Carbon Emissions: Evidence from the United States. *Energies* **2024**, *17*, 1748. [CrossRef]
25. Vishal, V.; Chandra, D.; Singh, U.; Verma, Y. Understanding Initial Opportunities and Key Challenges for CCUS Deployment in India at Scale. *Resour. Conserv. Recycl.* **2021**, *175*, 105829. [CrossRef]
26. IEA. *Direct Air Capture: A Key Technology for Net Zero*; OECD: Paris, France, 2022; ISBN 9789264585874.
27. Erans, M.; Sanz-Pérez, E.S.; Hanak, D.P.; Clulow, Z.; Reiner, D.M.; Mutch, G.A. Direct Air Capture: Process Technology, Techno-Economic and Socio-Political Challenges. *Energy Environ. Sci.* **2022**, *15*, 1360–1405. [CrossRef]
28. Gao, R.; Zhang, C.; Jun, K.-W.; Kim, S.K.; Park, H.-G.; Zhao, T.; Wang, L.; Wan, H.; Guan, G. Transformation of $CO_2$ into Liquid Fuels and Synthetic Natural Gas Using Green Hydrogen: A Comparative Analysis. *Fuel* **2021**, *291*, 120111. [CrossRef]
29. Kasturi, A.; Gug Jang, G.; Dona-Tella Akin, A.; Jackson, A.; Jun, J.; Stamberga, D.; Custelcean, R.; Sholl, D.S.; Yiacoumi, S.; Tsouris, C. An Effective Air–Liquid Contactor for $CO_2$ Direct Air Capture Using Aqueous Solvents. *Sep. Purif. Technol.* **2023**, *324*, 124398. [CrossRef]

30. Zhu, X.; Xie, W.; Wu, J.; Miao, Y.; Xiang, C.; Chen, C.; Ge, B.; Gan, Z.; Yang, F.; Zhang, M.; et al. Recent Advances in Direct Air Capture by Adsorption. *Chem. Soc. Rev.* **2022**, *51*, 6574–6651. [CrossRef] [PubMed]
31. Custelcean, R. Direct Air Capture of $CO_2$ Using Solvents. *Annu. Rev. Chem. Biomol. Eng.* **2022**, *13*, 217–234. [CrossRef]
32. Castro-Muñoz, R.; Zamidi Ahmad, M.; Malankowska, M.; Coronas, J. A New Relevant Membrane Application: $CO_2$ Direct Air Capture (DAC). *Chem. Eng. J.* **2022**, *446*, 137047. [CrossRef]
33. Fujikawa, S.; Selyanchyn, R.; Kunitake, T. A New Strategy for Membrane-Based Direct Air Capture. *Polym. J.* **2021**, *53*, 111–119. [CrossRef]
34. Lackner, K.S. Capture of Carbon Dioxide from Ambient Air. *Eur. Phys. J. Spec. Top.* **2009**, *176*, 93–106. [CrossRef]
35. Bisotti, F.; Hoff, K.A.; Mathisen, A.; Hovland, J. Direct Air Capture (DAC) Deployment: A Review of the Industrial Deployment. *Chem. Eng. Sci.* **2024**, *283*, 119416. [CrossRef]
36. An, K.; Li, K.; Yang, C.-M.; Brechtl, J.; Nawaz, K. A Comprehensive Review on Regeneration Strategies for Direct Air Capture. *J. CO2 Util.* **2023**, *76*, 102587. [CrossRef]
37. Ozkan, M.; Nayak, S.P.; Ruiz, A.D.; Jiang, W. Current Status and Pillars of Direct Air Capture Technologies. *iScience* **2022**, *25*, 103990. [CrossRef] [PubMed]
38. Chauvy, R.; Dubois, L. Life Cycle and Techno-economic Assessments of Direct Air Capture Processes: An Integrated Review. *Int. J. Energy Res.* **2022**, *46*, 10320–10344. [CrossRef]
39. McQueen, N.; Gomes, K.V.; McCormick, C.; Blumanthal, K.; Pisciotta, M.; Wilcox, J. A Review of Direct Air Capture (DAC): Scaling up Commercial Technologies and Innovating for the Future. *Prog. Energy* **2021**, *3*, 032001. [CrossRef]
40. Li, H.; Dilipkumar, A.; Abubakar, S.; Zhao, D. Covalent Organic Frameworks for $CO_2$ Capture: From Laboratory Curiosity to Industry Implementation. *Chem. Soc. Rev.* **2023**, *52*, 6294–6329. [CrossRef] [PubMed]
41. Keith, D.W.; Holmes, G.; St. Angelo, D.; Heidel, K. A Process for Capturing $CO_2$ from the Atmosphere. *Joule* **2018**, *2*, 1573–1594. [CrossRef]
42. Mostafa, M.; Antonicelli, C.; Varela, C.; Barletta, D.; Zondervan, E. Capturing $CO_2$ from the Atmosphere: Design and Analysis of a Large-Scale DAC Facility. *Carbon. Capture Sci. Technol.* **2022**, *4*, 100060. [CrossRef]
43. Wang, J.; Li, S.; Deng, S.; Zeng, X.; Li, K.; Liu, J.; Yan, J.; Lei, L. Energetic and Life Cycle Assessment of Direct Air Capture: A Review. *Sustain. Prod. Consum.* **2023**, *36*, 1–16. [CrossRef]
44. Elsener, B.; Addari, D.; Coray, S.; Rossi, A. Stainless Steel Reinforcing Bars—Reason for Their High Pitting Corrosion Resistance. *Mater. Corros.* **2011**, *62*, 111–119. [CrossRef]
45. Sequeira, C.A.C.; Cardoso, D.S.P.; Amaral, L.; Šljukić, B.; Santos, D.M.F. On the Performance of Commercially Available Corrosion-Resistant Nickel Alloys: A Review. *Corros. Rev.* **2016**, *34*, 187–200. [CrossRef]
46. Presuel-Moreno, F.; Jakab, M.A.; Tailleart, N.; Goldman, M.; Scully, J.R. Corrosion-Resistant Metallic Coatings. *Mater. Today* **2008**, *11*, 14–23. [CrossRef]
47. Holmes, G.; Keith, D.W. An Air–Liquid Contactor for Large-Scale Capture of $CO_2$ from Air. *Philos. Trans. R. Soc. A Math. Phys. Eng. Sci.* **2012**, *370*, 4380–4403. [CrossRef]
48. Prats-Salvado, E.; Jagtap, N.; Monnerie, N.; Sattler, C. Solar-Powered Direct Air Capture: Techno-Economic and Environmental Assessment. *Environ. Sci. Technol.* **2024**, *58*, 2282–2292. [CrossRef] [PubMed]
49. Nieves-Remacha, M.J.; Kulkarni, A.A.; Jensen, K.F. Gas–Liquid Flow and Mass Transfer in an Advanced-Flow Reactor. *Ind. Eng. Chem. Res.* **2013**, *52*, 8996–9010. [CrossRef]
50. Calautit, J.K.; Hughes, B.R. A Passive Cooling Wind Catcher with Heat Pipe Technology: CFD, Wind Tunnel and Field-Test Analysis. *Appl. Energy* **2016**, *162*, 460–471. [CrossRef]
51. Akinjide, J.; Lee, J.-Y.; Priye, A. Harnessing Wind with a Passive Direct Air Capture (PDAC) System for $CO_2$ Capture: Insights from Computational Fluid Dynamics Modeling. *Ind. Eng. Chem. Res.* **2023**, *62*, 18780–18791. [CrossRef]
52. Faisal Elmobarak, W.; Almomani, F.; Tawalbeh, M.; Al-Othman, A.; Martis, R.; Rasool, K. Current Status of $CO_2$ Capture with Ionic Liquids: Development and Progress. *Fuel* **2023**, *344*, 128102. [CrossRef]
53. Bak, C.; Asif, M.; Kim, W.-S. Experimental Study on $CO_2$ Capture by Chilled Ammonia Process. *Chem. Eng. J.* **2015**, *265*, 1–8. [CrossRef]
54. Chehrazi, M.; Moghadas, B.K. A Review on $CO_2$ Capture with Chilled Ammonia and $CO_2$ Utilization in Urea Plant. *J. CO2 Util.* **2022**, *61*, 102030. [CrossRef]
55. Darde, V.; Thomsen, K.; van Well, W.J.M.; Stenby, E.H. Chilled Ammonia Process for $CO_2$ Capture. *Energy Procedia* **2009**, *1*, 1035–1042. [CrossRef]
56. Perry, R.J. Aminosilicone Systems for Post-Combustion $CO_2$ Capture. In *Absorption-Based Post-combustion Capture of Carbon Dioxide*; Elsevier: Amsterdam, The Netherlands, 2016; pp. 121–144.
57. Westendorf, T.; Farnum, R.; Rubinsztajn, G.; Wood, B.; Perry, R.; McDermott, J.; Enick, R.; Tapriyal, D. Measurement of $CO_2$ Diffusivity in Phase-Changing Aminosilicone $CO_2$ Capture Solvent. *Energy Fuels* **2018**, *32*, 6901–6909. [CrossRef]
58. Perry, R.J.; Grocela-Rocha, T.A.; O'Brien, M.J.; Genovese, S.; Wood, B.R.; Lewis, L.N.; Lam, H.; Soloveichik, G.; Rubinsztajn, M.; Kniajanski, S.; et al. Aminosilicone Solvents for $CO_2$ Capture. *ChemSusChem* **2010**, *3*, 919–930. [CrossRef] [PubMed]
59. Soltani, S.M.; Fennell, P.S.; Mac Dowell, N. A Parametric Study of $CO_2$ Capture from Gas-Fired Power Plants Using Monoethanolamine (MEA). *Int. J. Greenh. Gas Control* **2017**, *63*, 321–328. [CrossRef]

60. Li, K.; Leigh, W.; Feron, P.; Yu, H.; Tade, M. Systematic Study of Aqueous Monoethanolamine (MEA)-Based $CO_2$ Capture Process: Techno-Economic Assessment of the MEA Process and Its Improvements. *Appl. Energy* **2016**, *165*, 648–659. [CrossRef]
61. Luis, P. Use of Monoethanolamine (MEA) for $CO_2$ Capture in a Global Scenario: Consequences and Alternatives. *Desalination* **2016**, *380*, 93–99. [CrossRef]
62. Rochelle, G.T. Amine Scrubbing for $CO_2$ Capture. *Science* **2009**, *325*, 1652–1654. [CrossRef]
63. Tamajón, F.J.; Álvarez, E.; Cerdeira, F.; Gómez-Díaz, D. $CO_2$ Absorption into N-Methyldiethanolamine Aqueous-Organic Solvents. *Chem. Eng. J.* **2016**, *283*, 1069–1080. [CrossRef]
64. Khan, S.N.; Hailegiorgis, S.M.; Man, Z.; Shariff, A.M.; Garg, S. Thermophysical Properties of Concentrated Aqueous Solution of N -Methyldiethanolamine (MDEA), Piperazine (PZ), and Ionic Liquids Hybrid Solvent for $CO_2$ Capture. *J. Mol. Liq.* **2017**, *229*, 221–229. [CrossRef]
65. Fu, D.; Zhang, P. Investigation of the Absorption Performance and Viscosity for $CO_2$ Capture Process Using [Bmim][Gly] Promoted MDEA (N-Methyldiethanolamine) Aqueous Solution. *Energy* **2015**, *87*, 165–172. [CrossRef]
66. Zhang, Z.; Yan, Y.; Chen, Y.; Zhang, L. Investigation of $CO_2$ Absorption in Methyldiethanolamine and 2-(1-Piperazinyl)-Ethylamine Using Hollow Fiber Membrane Contactors: Part C. Effect of Operating Variables. *J. Nat. Gas. Sci. Eng.* **2014**, *20*, 58–66. [CrossRef]
67. Brennecke, J.F.; Gurkan, B.E. Ionic Liquids for $CO_2$ Capture and Emission Reduction. *J. Phys. Chem. Lett.* **2010**, *1*, 3459–3464. [CrossRef]
68. Vaidya, P.D.; Kenig, E.Y. $CO_2$—Alkanolamine Reaction Kinetics: A Review of Recent Studies. *Chem. Eng. Technol.* **2007**, *30*, 1467–1474. [CrossRef]
69. Ramdin, M.; de Loos, T.W.; Vlugt, T.J.H. State-of-the-Art of $CO_2$ Capture with Ionic Liquids. *Ind. Eng. Chem. Res.* **2012**, *51*, 8149–8177. [CrossRef]
70. Majeed, H.; Svendsen, H.F. Characterization of Aerosol Emissions from $CO_2$ Capture Plants Treating Various Power Plant and Industrial Flue Gases. *Int. J. Greenh. Gas Control* **2018**, *74*, 282–295. [CrossRef]
71. Yi, N.; Fang, M.; Di, W.; Xia, Z.; Wang, T.; Wang, Q. Aerosol Emissions of Amine-Based $CO_2$ Absorption System: Effects of Condensation Nuclei and Operating Conditions. *Environ. Sci. Technol.* **2021**, *55*, 5152–5160. [CrossRef] [PubMed]
72. Yu, X.; Wu, H.; Li, W.; Zhang, Q.; Yang, H. Formation Mechanisms and Emission Characteristics of Aerosol in $CO_2$ Capture by Chemical Absorption Based on Ethanolamine Solution. *Energy Fuels* **2024**, *38*, 6230–6237. [CrossRef]
73. Mazari, S.A.; Alaba, P.; Saeed, I.M. Formation and Elimination of Nitrosamines and Nitramines in Freshwaters Involved in Post-Combustion Carbon Capture Process. *J. Environ. Chem. Eng.* **2019**, *7*, 103111. [CrossRef]
74. Yu, K.; Mitch, W.A.; Dai, N. Nitrosamines and Nitramines in Amine-Based Carbon Dioxide Capture Systems: Fundamentals, Engineering Implications, and Knowledge Gaps. *Environ. Sci. Technol.* **2017**, *51*, 11522–11536. [CrossRef]
75. Chen, X.; Huang, G.; An, C.; Yao, Y.; Zhao, S. Emerging N-Nitrosamines and N-Nitramines from Amine-Based Post-Combustion $CO_2$ Capture—A Review. *Chem. Eng. J.* **2018**, *335*, 921–935. [CrossRef]
76. Corvo, M.C.; Sardinha, J.; Casimiro, T.; Marin, G.; Seferin, M.; Einloft, S.; Menezes, S.C.; Dupont, J.; Cabrita, E.J. A Rational Approach to $CO_2$ Capture by Imidazolium Ionic Liquids: Tuning $CO_2$ Solubility by Cation Alkyl Branching. *ChemSusChem* **2015**, *8*, 1935–1946. [CrossRef]
77. Palomar, J.; Gonzalez-Miquel, M.; Polo, A.; Rodriguez, F. Understanding the Physical Absorption of $CO_2$ in Ionic Liquids Using the COSMO-RS Method. *Ind. Eng. Chem. Res.* **2011**, *50*, 3452–3463. [CrossRef]
78. Kazarian, S.G.; Briscoe, B.J.; Welton, T. Combining Ionic Liquids and Supercritical Fluids: In Situ ATR-IR Study of $CO_2$ Dissolved in Two Ionic Liquids at High Pressures. *Chem. Commun.* **2000**, *20*, 2047–2048. [CrossRef]
79. Cadena, C.; Anthony, J.L.; Shah, J.K.; Morrow, T.I.; Brennecke, J.F.; Maginn, E.J. Why Is $CO_2$ So Soluble in Imidazolium-Based Ionic Liquids? *J. Am. Chem. Soc.* **2004**, *126*, 5300–5308. [CrossRef]
80. Anthony, J.L.; Anderson, J.L.; Maginn, E.J.; Brennecke, J.F. Anion Effects on Gas Solubility in Ionic Liquids. *J. Phys. Chem. B* **2005**, *109*, 6366–6374. [CrossRef] [PubMed]
81. Aki, S.N.; Mellein, B.R.; Saurer, E.M.; Brennecke, J.F. High-Pressure Phase Behavior of Carbon Dioxide with Imidazolium-Based Ionic Liquids. *J. Phys. Chem. B* **2004**, *108*, 20355–20365. [CrossRef]
82. Almantariotis, D.; Gefflaut, T.; Pádua, A.A.H.; Coxam, J.-Y.; Costa Gomes, M.F. Effect of Fluorination and Size of the Alkyl Side-Chain on the Solubility of Carbon Dioxide in 1-Alkyl-3-Methylimidazolium Bis(Trifluoromethylsulfonyl)Amide Ionic Liquids. *J. Phys. Chem. B* **2010**, *114*, 3608–3617. [CrossRef]
83. Bates, E.D.; Mayton, R.D.; Ntai, I.; Davis, J.H. $CO_2$ Capture by a Task-Specific Ionic Liquid. *J. Am. Chem. Soc.* **2002**, *124*, 926–927. [CrossRef]
84. Gurkan, B.E.; de la Fuente, J.C.; Mindrup, E.M.; Ficke, L.E.; Goodrich, B.F.; Price, E.A.; Schneider, W.F.; Brennecke, J.F. Equimolar $CO_2$ Absorption by Anion-Functionalized Ionic Liquids. *J. Am. Chem. Soc.* **2010**, *132*, 2116–2117. [CrossRef] [PubMed]
85. Taheri, M.; Dai, C.; Lei, Z. $CO_2$ Capture by Methanol, Ionic Liquid, and Their Binary Mixtures: Experiments, Modeling, and Process Simulation. *AIChE J.* **2018**, *64*, 2168–2180. [CrossRef]
86. Klähn, M.; Seduraman, A. What Determines $CO_2$ Solubility in Ionic Liquids? A Molecular Simulation Study. *J. Phys. Chem. B* **2015**, *119*, 10066–10078. [CrossRef]
87. Ma, T.; Wang, J.; Du, Z.; Abdeltawab, A.A.; Al-Enizi, A.M.; Chen, X.; Yu, G. A Process Simulation Study of $CO_2$ Capture by Ionic Liquids. *Int. J. Greenh. Gas Control* **2017**, *58*, 223–231. [CrossRef]

88. Uludag-Demirer, S.; Smerigan, A.; Hsiao, P.; Marks, A.; Smith, M.R.; Liao, W. Enhanced Carbon Dioxide Capture Using a Mixed Amino Acid Salt Solution. *Ind. Eng. Chem. Res.* **2023**, *62*, 4064–4072. [CrossRef]
89. Rahim, N.A.; Ghasem, N.; Al-Marzouqi, M. Absorption of $CO_2$ from Natural Gas Using Different Amino Acid Salt Solutions and Regeneration Using Hollow Fiber Membrane Contactors. *J. Nat. Gas Sci. Eng.* **2015**, *26*, 108–117. [CrossRef]
90. Xu, X.; Myers, M.B.; Versteeg, F.G.; Adam, E.; White, C.; Crooke, E.; Wood, C.D. Next Generation Amino Acid Technology for $CO_2$ Capture. *J. Mater. Chem. A Mater.* **2021**, *9*, 1692–1704. [CrossRef]
91. Zhang, Z.; Li, Y.; Zhang, W.; Wang, J.; Soltanian, M.R.; Olabi, A.G. Effectiveness of Amino Acid Salt Solutions in Capturing $CO_2$: A Review. *Renew. Sustain. Energy Rev.* **2018**, *98*, 179–188. [CrossRef]
92. Beuttler, C.; Charles, L.; Wurzbacher, J. The Role of Direct Air Capture in Mitigation of Anthropogenic Greenhouse Gas Emissions. *Front. Clim.* **2019**, *1*, 10. [CrossRef]
93. You, J.K.; Park, H.; Yang, S.H.; Hong, W.H.; Shin, W.; Kang, J.K.; Yi, K.B.; Kim, J.-N. Influence of Additives Including Amine and Hydroxyl Groups on Aqueous Ammonia Absorbent for $CO_2$ Capture. *J. Phys. Chem. B* **2008**, *112*, 4323–4328. [CrossRef]
94. Hou, C.; Kumar, D.R.; Jin, Y.; Wu, Y.; Lee, J.J.; Jones, C.W.; Wang, T. Porosity and Hydrophilicity Modulated Quaternary Ammonium-Based Sorbents for $CO_2$ Capture. *Chem. Eng. J.* **2021**, *413*, 127532. [CrossRef]
95. Park, D.J.; Choi, J.H.; Kim, Y.E.; Nam, S.C.; Lee, K.B.; Yoon, Y. Il Chemical Absorption of Carbon Dioxide Using Aqueous Piperidine Derivatives. *Chem. Eng. Technol.* **2017**, *40*, 2266–2273. [CrossRef]
96. Sayari, A.; Heydari-Gorji, A.; Yang, Y. $CO_2$—Induced Degradation of Amine-Containing Adsorbents: Reaction Products and Pathways. *J. Am. Chem. Soc.* **2012**, *134*, 13834–13842. [CrossRef] [PubMed]
97. Heydari-Gorji, A.; Belmabkhout, Y.; Sayari, A. Degradation of Amine-Supported $CO_2$ Adsorbents in the Presence of Oxygen-Containing Gases. *Microporous Mesoporous Mater.* **2011**, *145*, 146–149. [CrossRef]
98. Choi, S.; Gray, M.L.; Jones, C.W. Amine-Tethered Solid Adsorbents Coupling High Adsorption Capacity and Regenerability for $CO_2$ Capture from Ambient Air. *ChemSusChem* **2011**, *4*, 628–635. [CrossRef] [PubMed]
99. Alkhabbaz, M.A.; Khunsupat, R.; Jones, C.W. Guanidinylated Poly(Allylamine) Supported on Mesoporous Silica for $CO_2$ Capture from Flue Gas. *Fuel* **2014**, *121*, 79–85. [CrossRef]
100. Chaikittisilp, W.; Khunsupat, R.; Chen, T.T.; Jones, C.W. Poly(Allylamine)–Mesoporous Silica Composite Materials for $CO_2$ Capture from Simulated Flue Gas or Ambient Air. *Ind. Eng. Chem. Res.* **2011**, *50*, 14203–14210. [CrossRef]
101. Sujan, A.R.; Kumar, D.R.; Sakwa-Novak, M.; Ping, E.W.; Hu, B.; Park, S.J.; Jones, C.W. Poly(Glycidyl Amine)-Loaded SBA-15 Sorbents for $CO_2$ Capture from Dilute and Ultradilute Gas Mixtures. *ACS Appl. Polym. Mater.* **2019**, *1*, 3137–3147. [CrossRef]
102. Park, S.J.; Lee, J.J.; Hoyt, C.B.; Kumar, D.R.; Jones, C.W. Silica Supported Poly(Propylene Guanidine) as a $CO_2$ Sorbent in Simulated Flue Gas and Direct Air Capture. *Adsorption* **2020**, *26*, 89–101. [CrossRef]
103. Hamdy, L.B.; Goel, C.; Rudd, J.A.; Barron, A.R.; Andreoli, E. The Application of Amine-Based Materials for Carbon Capture and Utilisation: An Overarching View. *Mater. Adv.* **2021**, *2*, 5843–5880. [CrossRef]
104. Irani, M.; Jacobson, A.T.; Gasem, K.A.M.; Fan, M. Modified Carbon Nanotubes/Tetraethylenepentamine for $CO_2$ Capture. *Fuel* **2017**, *206*, 10–18. [CrossRef]
105. Fisher, J.C.; Tanthana, J.; Chuang, S.S.C. Oxide-supported Tetraethylenepentamine for $CO_2$ Capture. *Environ. Prog. Sustain. Energy* **2009**, *28*, 589–598. [CrossRef]
106. Miao, Y.; Wang, Y.; Ge, B.; He, Z.; Zhu, X.; Li, J.; Liu, S.; Yu, L. Mixed Diethanolamine and Polyethyleneimine with Enhanced $CO_2$ Capture Capacity from Air. *Adv. Sci.* **2023**, *10*, 2207253. [CrossRef] [PubMed]
107. Al-Absi, A.A.; Benneker, A.M.; Mahinpey, N. Ambient and Sub-Ambient Temperature Direct Air $CO_2$ Capture (DAC) by Novel Supported in Situ Polymerized Amines. *J. Mater. Chem. A Mater.* **2024**, *12*, 10507–10527. [CrossRef]
108. Zhang, W.; Liu, H.; Sun, C.; Drage, T.C.; Snape, C.E. Capturing $CO_2$ from Ambient Air Using a Polyethyleneimine–Silica Adsorbent in Fluidized Beds. *Chem. Eng. Sci.* **2014**, *116*, 306–316. [CrossRef]
109. Sayari, A.; Liu, Q.; Mishra, P. Enhanced Adsorption Efficiency through Materials Design for Direct Air Capture over Supported Polyethylenimine. *ChemSusChem* **2016**, *9*, 2796–2803. [CrossRef]
110. Heydari-Gorji, A.; Belmabkhout, Y.; Sayari, A. Polyethylenimine-Impregnated Mesoporous Silica: Effect of Amine Loading and Surface Alkyl Chains on $CO_2$ Adsorption. *Langmuir* **2011**, *27*, 12411–12416. [CrossRef] [PubMed]
111. Chue, K.T.; Kim, J.N.; Yoo, Y.J.; Cho, S.H.; Yang, R.T. Comparison of Activated Carbon and Zeolite 13X for $CO_2$ Recovery from Flue Gas by Pressure Swing Adsorption. *Ind. Eng. Chem. Res.* **1995**, *34*, 591–598. [CrossRef]
112. Sreńscek-Nazzal, J.; Kiełbasa, K. Advances in Modification of Commercial Activated Carbon for Enhancement of $CO_2$ Capture. *Appl. Surf. Sci.* **2019**, *494*, 137–151. [CrossRef]
113. Abuelnoor, N.; AlHajaj, A.; Khaleel, M.; Vega, L.F.; Abu-Zahra, M.R.M. Activated Carbons from Biomass-Based Sources for $CO_2$ Capture Applications. *Chemosphere* **2021**, *282*, 131111. [CrossRef]
114. Creamer, A.E.; Gao, B. Carbon-Based Adsorbents for Postcombustion $CO_2$ Capture: A Critical Review. *Environ. Sci. Technol.* **2016**, *50*, 7276–7289. [CrossRef] [PubMed]
115. Zhang, Z.; Cano, Z.P.; Luo, D.; Dou, H.; Yu, A.; Chen, Z. Rational Design of Tailored Porous Carbon-Based Materials for $CO_2$ Capture. *J. Mater. Chem. A Mater.* **2019**, *7*, 20985–21003. [CrossRef]
116. Kumar, S.; Srivastava, R.; Koh, J. Utilization of Zeolites as $CO_2$ Capturing Agents: Advances and Future Perspectives. *J. CO2 Util.* **2020**, *41*, 101251. [CrossRef]

117. Krishna, R.; van Baten, J.M. A Comparison of the $CO_2$ Capture Characteristics of Zeolites and Metal–Organic Frameworks. *Sep. Purif. Technol.* **2012**, *87*, 120–126. [CrossRef]
118. Cecilia, J.A.; Vilarrasa-García, E.; Morales-Ospino, R.; Finocchio, E.; Busca, G.; Sapag, K.; Villarroel-Rocha, J.; Bastos-Neto, M.; Azevedo, D.C.S.; Rodríguez-Castellón, E. Kaolinite-Based Zeolites Synthesis and Their Application in $CO_2$ Capture Processes. *Fuel* **2022**, *320*, 123953. [CrossRef]
119. Sun, Q.; Li, Z.; Searles, D.J.; Chen, Y.; Lu, G.; Du, A. Charge-Controlled Switchable $CO_2$ Capture on Boron Nitride Nanomaterials. *J. Am. Chem. Soc.* **2013**, *135*, 8246–8253. [CrossRef] [PubMed]
120. Liang, J.; Song, Q.; Lin, J.; Li, G.; Fang, Y.; Guo, Z.; Huang, Y.; Lee, C.-S.; Tang, C. In Situ Cu-Loaded Porous Boron Nitride Nanofiber as an Efficient Adsorbent for $CO_2$ Capture. *ACS Sustain. Chem. Eng.* **2020**, *8*, 7454–7462. [CrossRef]
121. Yang, C.; Liu, D.; Chen, Y.; Chen, C.; Wang, J.; Fan, Y.; Huang, S.; Lei, W. Three-Dimensional Functionalized Boron Nitride Nanosheets/ZnO Superstructures for $CO_2$ Capture. *ACS Appl. Mater. Interfaces* **2019**, *11*, 10276–10282. [CrossRef]
122. Amaraweera, S.M.; Gunathilake, C.A.; Gunawardene, O.H.P.; Dassanayake, R.S.; Cho, E.-B.; Du, Y. Carbon Capture Using Porous Silica Materials. *Nanomaterials* **2023**, *13*, 2050. [CrossRef] [PubMed]
123. Vittoni, C.; Gatti, G.; Paul, G.; Mangano, E.; Brandani, S.; Bisio, C.; Marchese, L. Non-Porous versus Mesoporous Siliceous Materials for $CO_2$ Capture. *ChemistryOpen* **2019**, *8*, 719–727. [CrossRef]
124. Abd, A.A.; Othman, M.R.; Kim, J. A Review on Application of Activated Carbons for Carbon Dioxide Capture: Present Performance, Preparation, and Surface Modification for Further Improvement. *Environ. Sci. Pollut. Res.* **2021**, *28*, 43329–43364. [CrossRef] [PubMed]
125. Zaker, A.; ben Hammouda, S.; Sun, J.; Wang, X.; Li, X.; Chen, Z. Carbon-Based Materials for $CO_2$ Capture: Their Production, Modification and Performance. *J. Environ. Chem. Eng.* **2023**, *11*, 109741. [CrossRef]
126. Ghanbari, T.; Abnisa, F.; Wan Daud, W.M.A. A Review on Production of Metal Organic Frameworks (MOF) for $CO_2$ Adsorption. *Sci. Total Environ.* **2020**, *707*, 135090. [CrossRef] [PubMed]
127. Zhuang, W.; Yuan, D.; Liu, D.; Zhong, C.; Li, J.-R.; Zhou, H.-C. Robust Metal–Organic Framework with An Octatopic Ligand for Gas Adsorption and Separation: Combined Characterization by Experiments and Molecular Simulation. *Chem. Mater.* **2012**, *24*, 18–25. [CrossRef]
128. Bae, Y.-S.; Mulfort, K.L.; Frost, H.; Ryan, P.; Punnathanam, S.; Broadbelt, L.J.; Hupp, J.T.; Snurr, R.Q. Separation of $CO_2$ from $CH_4$ Using Mixed-Ligand Metal−Organic Frameworks. *Langmuir* **2008**, *24*, 8592–8598. [CrossRef] [PubMed]
129. Wu, M.-X.; Yang, Y.-W. Applications of Covalent Organic Frameworks (COFs): From Gas Storage and Separation to Drug Delivery. *Chin. Chem. Lett.* **2017**, *28*, 1135–1143. [CrossRef]
130. Lyu, H.; Li, H.; Hanikel, N.; Wang, K.; Yaghi, O.M. Covalent Organic Frameworks for Carbon Dioxide Capture from Air. *J. Am. Chem. Soc.* **2022**, *144*, 12989–12995. [CrossRef] [PubMed]
131. Song, K.S.; Fritz, P.W.; Coskun, A. Porous Organic Polymers for $CO_2$ Capture, Separation and Conversion. *Chem. Soc. Rev.* **2022**, *51*, 9831–9852. [CrossRef] [PubMed]
132. Tian, Y.; Zhu, G. Porous Aromatic Frameworks (PAFs). *Chem. Rev.* **2020**, *120*, 8934–8986. [CrossRef]
133. Babarao, R.; Dai, S.; Jiang, D. Functionalizing Porous Aromatic Frameworks with Polar Organic Groups for High-Capacity and Selective $CO_2$ Separation: A Molecular Simulation Study. *Langmuir* **2011**, *27*, 3451–3460. [CrossRef]
134. Yu, C.; Wang, Y.; Xia, Y.; Luo, S.; Ma, X.; Yin, B.H.; Wang, X. Polymers of Intrinsic Microporosity with Internal Dihedral Lock for Efficient Gas Separation. *Adv. Membr.* **2024**, *4*, 100097. [CrossRef]
135. Arabi Shamsabadi, A.; Rezakazemi, M.; Seidi, F.; Riazi, H.; Aminabhavi, T.; Soroush, M. Next Generation Polymers of Intrinsic Microporosity with Tunable Moieties for Ultrahigh Permeation and Precise Molecular $CO_2$ Separation. *Prog. Energy Combust. Sci.* **2021**, *84*, 100903. [CrossRef]
136. Yan, Q.; Lin, Y.; Wu, P.; Zhao, L.; Cao, L.; Peng, L.; Kong, C.; Chen, L. Designed Synthesis of Functionalized Two-Dimensional Metal–Organic Frameworks with Preferential $CO_2$ Capture. *Chempluschem* **2013**, *78*, 86–91. [CrossRef]
137. Chakraborty, G.; Das, P.; Mandal, S.K. Efficient and Highly Selective $CO_2$ Capture, Separation, and Chemical Conversion under Ambient Conditions by a Polar-Group-Appended Copper(II) Metal–Organic Framework. *Inorg. Chem.* **2021**, *60*, 5071–5080. [CrossRef]
138. Khan, N.A.; Jhung, S.H. Adsorptive Removal and Separation of Chemicals with Metal-Organic Frameworks: Contribution of $\pi$-Complexation. *J. Hazard. Mater.* **2017**, *325*, 198–213. [CrossRef] [PubMed]
139. Gupta, V.; Mandal, S.K. Effect of Unsaturated Metal Site Modulation in Highly Stable Microporous Materials on $CO_2$ Capture and Fixation. *Inorg. Chem.* **2022**, *61*, 3086–3096. [CrossRef]
140. Kökçam-Demir, Ü.; Goldman, A.; Esrafili, L.; Gharib, M.; Morsali, A.; Weingart, O.; Janiak, C. Coordinatively Unsaturated Metal Sites (Open Metal Sites) in Metal–Organic Frameworks: Design and Applications. *Chem. Soc. Rev.* **2020**, *49*, 2751–2798. [CrossRef] [PubMed]
141. Zhai, L.; Yao, Y.; Ma, B.; Hasan, M.M.; Han, Y.; Mi, L.; Nagao, Y.; Li, Z. Accumulation of Sulfonic Acid Groups Anchored in Covalent Organic Frameworks as an Intrinsic Proton-Conducting Electrolyte. *Macromol. Rapid Commun.* **2022**, *43*, 2100590. [CrossRef]
142. Liu, J.; Wang, N.; Ma, L. Recent Advances in Covalent Organic Frameworks for Catalysis. *Chem. Asian J.* **2020**, *15*, 338–351. [CrossRef]

143. Sahoo, R.; Mondal, S.; Pal, S.C.; Mukherjee, D.; Das, M.C. Covalent-Organic Frameworks (COFs) as Proton Conductors. *Adv. Energy Mater.* **2021**, *11*, 2102300. [CrossRef]
144. Duong, P.H.H.; Shin, Y.K.; Kuehl, V.A.; Afroz, M.M.; Hoberg, J.O.; Parkinson, B.; van Duin, A.C.T.; Li-Oakey, K.D. Molecular Interactions and Layer Stacking Dictate Covalent Organic Framework Effective Pore Size. *ACS Appl. Mater. Interfaces* **2021**, *13*, 42164–42175. [CrossRef] [PubMed]
145. Deng, L.; Ding, Z.; Ye, X.; Jiang, D. Covalent Organic Frameworks: Chemistry of Pore Interface and Wall Surface Perturbation and Impact on Functions. *Acc. Mater. Res.* **2022**, *3*, 879–893. [CrossRef]
146. Buyukcakir, O.; Seo, Y.; Coskun, A. Thinking Outside the Cage: Controlling the Extrinsic Porosity and Gas Uptake Properties of Shape-Persistent Molecular Cages in Nanoporous Polymers. *Chem. Mater.* **2015**, *27*, 4149–4155. [CrossRef]
147. Je, S.H.; Buyukcakir, O.; Kim, D.; Coskun, A. Direct Utilization of Elemental Sulfur in the Synthesis of Microporous Polymers for Natural Gas Sweetening. *Chem* **2016**, *1*, 482–493. [CrossRef]
148. Patel, H.A.; Je, S.H.; Park, J.; Jung, Y.; Coskun, A.; Yavuz, C.T. Directing the Structural Features of $N_2$—Phobic Nanoporous Covalent Organic Polymers for $CO_2$ Capture and Separation. *Chem—A Eur. J.* **2014**, *20*, 772–780. [CrossRef] [PubMed]
149. Song, K.S.; Kim, D.; Polychronopoulou, K.; Coskun, A. Synthesis of Highly Porous Coordination Polymers with Open Metal Sites for Enhanced Gas Uptake and Separation. *ACS Appl. Mater. Interfaces* **2016**, *8*, 26860–26867. [CrossRef]
150. Zhang, P.; Zhang, C.; Wang, L.; Dong, J.; Gai, D.; Wang, W.; Nguyen, T.S.; Yavuz, C.T.; Zou, X.; Zhu, G. Basic Alkylamine Functionalized PAF-1 Hybrid Membrane with High Compatibility for Superior $CO_2$ Separation from Flue Gas. *Adv. Funct. Mater.* **2023**, *33*, 2210091. [CrossRef]
151. Lu, W.; Yuan, D.; Sculley, J.; Zhao, D.; Krishna, R.; Zhou, H.-C. Sulfonate-Grafted Porous Polymer Networks for Preferential $CO_2$ Adsorption at Low Pressure. *J. Am. Chem. Soc.* **2011**, *133*, 18126–18129. [CrossRef] [PubMed]
152. Vopička, O.; Friess, K.; Hynek, V.; Sysel, P.; Zgažar, M.; Šípek, M.; Pilnáček, K.; Lanč, M.; Jansen, J.C.; Mason, C.R.; et al. Equilibrium and Transient Sorption of Vapours and Gases in the Polymer of Intrinsic Microporosity PIM-1. *J. Memb. Sci.* **2013**, *434*, 148–160. [CrossRef]
153. Wang, X.; Guo, H.; Yu, C.; Jing, Y.; Han, Z.; Ma, X.; Yang, C.; Liu, M.; Zhai, D.; Zheng, D.; et al. Practical Enantioselective Synthesis of Chiroptical Polymers of Intrinsic Microporosity with Circular Polarized Luminescence. *Macromolecules* **2021**, *54*, 11180–11186. [CrossRef]
154. Voskian, S.; Hatton, T.A. Faradaic Electro-Swing Reactive Adsorption for $CO_2$ Capture. *Energy Environ. Sci.* **2019**, *12*, 3530–3547. [CrossRef]
155. Gurkan, B.; Simeon, F.; Hatton, T.A. Quinone Reduction in Ionic Liquids for Electrochemical $CO_2$ Separation. *ACS Sustain. Chem. Eng.* **2015**, *3*, 1394–1405. [CrossRef]
156. Ranjan, R.; Olson, J.; Singh, P.; Lorance, E.D.; Buttry, D.A.; Gould, I.R. Reversible Electrochemical Trapping of Carbon Dioxide Using 4,4′-Bipyridine That Does Not Require Thermal Activation. *J. Phys. Chem. Lett.* **2015**, *6*, 4943–4946. [CrossRef]
157. Rheinhardt, J.H.; Singh, P.; Tarakeshwar, P.; Buttry, D.A. Electrochemical Capture and Release of Carbon Dioxide. *ACS Energy Lett.* **2017**, *2*, 454–461. [CrossRef]
158. Singh, P.; Rheinhardt, J.H.; Olson, J.Z.; Tarakeshwar, P.; Mujica, V.; Buttry, D.A. Electrochemical Capture and Release of Carbon Dioxide Using a Disulfide–Thiocarbonate Redox Cycle. *J. Am. Chem. Soc.* **2017**, *139*, 1033–1036. [CrossRef] [PubMed]
159. Hatton, T.A.; Voskian, S. Electro-Swing Adsorption for $CO_2$ Emissions Mitigation—From Concept to Start-Up. *ECS Meet. Abstr.* **2023**, *MA2023-01*, 1760. [CrossRef]
160. Wilcox, J. An Electro-Swing Approach. *Nat. Energy* **2020**, *5*, 121–122. [CrossRef]
161. Biery, A.R.; Shokrollahzadeh Behbahani, H.; Green, M.D.; Knauss, D.M. Polydiallylammonium-Polysulfone Multiblock Copolymers for Moisture-Swing Direct Air Capture of Carbon Dioxide. *ACS Appl. Polym. Mater.* **2024**, *6*, 2649–2658. [CrossRef]
162. Wang, T.; Lackner, K.S.; Wright, A.B. Moisture-Swing Sorption for Carbon Dioxide Capture from Ambient Air: A Thermodynamic Analysis. *Phys. Chem. Chem. Phys.* **2013**, *15*, 504–514. [CrossRef]
163. Fasihi, M.; Efimova, O.; Breyer, C. Techno-Economic Assessment of $CO_2$ Direct Air Capture Plants. *J. Clean. Prod.* **2019**, *224*, 957–980. [CrossRef]
164. Hou, C.; Wu, Y.; Jiao, Y.; Huang, J.; Wang, T.; Fang, M.; Zhou, H. Integrated Direct Air Capture and $CO_2$ Utilization of Gas Fertilizer Based on Moisture Swing Adsorption. *J. Zhejiang Univ.-Sci. A* **2017**, *18*, 819–830. [CrossRef]
165. Shi, X.; Xiao, H.; Kanamori, K.; Yonezu, A.; Lackner, K.S.; Chen, X. Moisture-Driven $CO_2$ Sorbents. *Joule* **2020**, *4*, 1823–1837. [CrossRef]
166. Shi, X.; Xiao, H.; Liao, X.; Armstrong, M.; Chen, X.; Lackner, K.S. Humidity Effect on Ion Behaviors of Moisture-Driven $CO_2$ Sorbents. *J. Chem. Phys.* **2018**, *149*, 164708. [CrossRef] [PubMed]
167. Wang, T.; Wang, X.; Hou, C.; Liu, J. Quaternary Functionalized Mesoporous Adsorbents for Ultra-High Kinetics of $CO_2$ Capture from Air. *Sci. Rep.* **2020**, *10*, 21429. [CrossRef] [PubMed]
168. Li, G.; Yao, J. Snap-Off during Imbibition in Porous Media: Mechanisms, Influencing Factors, and Impacts. *Eng* **2023**, *4*, 2896–2925. [CrossRef]
169. Yao, J.; Oakey, J. Geometrically-Mediated Snap-off of Water-in-Oil Emulsion Droplets in Microfluidic Flow Focusing Devices. *J. Oil Gas Petrochem. Sci.* **2018**, *1*, 42. [CrossRef] [PubMed]
170. Yao, J. A Microfluidic Model for Visualizing Snap-off During Imbibition. Ph.D. Dissertation, University of Wyoming, Laramie, WY, USA, 2017.

171. Qu, Z.; Yao, J.; Yang, Y.; Wang, B.; He, L. Laboratory Experiments of a Microfluidic Model for Imbibition. *J. Petrochem. Univ.* **2014**, *37*, 64–66.
172. Fu, Q.; Halim, A.; Kim, J.; Scofield, J.M.P.; Gurr, P.A.; Kentish, S.E.; Qiao, G.G. Highly Permeable Membrane Materials for $CO_2$ Capture. *J. Mater. Chem. A Mater.* **2013**, *1*, 13769. [CrossRef]
173. Merkel, T.C.; Lin, H.; Wei, X.; Baker, R. Power Plant Post-Combustion Carbon Dioxide Capture: An Opportunity for Membranes. *J. Memb. Sci.* **2010**, *359*, 126–139. [CrossRef]
174. Yoo, M.J.; Kim, K.H.; Lee, J.H.; Kim, T.W.; Chung, C.W.; Cho, Y.H.; Park, H.B. Ultrathin Gutter Layer for High-Performance Thin-Film Composite Membranes for $CO_2$ Separation. *J. Memb. Sci.* **2018**, *566*, 336–345. [CrossRef]
175. Lin, H.; Van Wagner, E.; Freeman, B.D.; Toy, L.G.; Gupta, R.P. Plasticization-Enhanced Hydrogen Purification Using Polymeric Membranes. *Science* **2006**, *311*, 639–642. [CrossRef] [PubMed]
176. Li, S.; Wang, Z.; Zhang, C.; Wang, M.; Yuan, F.; Wang, J.; Wang, S. Interfacially Polymerized Thin Film Composite Membranes Containing Ethylene Oxide Groups for $CO_2$ Separation. *J. Memb. Sci.* **2013**, *436*, 121–131. [CrossRef]
177. Fujikawa, S.; Ariyoshi, M.; Selyanchyn, R.; Kunitake, T. Ultra-Fast, Selective $CO_2$ Permeation by Free-Standing Siloxane Nanomembranes. *Chem. Lett.* **2019**, *48*, 1351–1354. [CrossRef]
178. Das, M.; Perry, J.D.; Koros, W.J. Gas-Transport-Property Performance of Hybrid Carbon Molecular Sieve−Polymer Materials. *Ind. Eng. Chem. Res.* **2010**, *49*, 9310–9321. [CrossRef]
179. Clarizia, G.; Algieri, C.; Regina, A.; Drioli, E. Zeolite-Based Composite PEEK-WC Membranes: Gas Transport and Surface Properties. *Microporous Mesoporous Mater.* **2008**, *115*, 67–74. [CrossRef]
180. Li, Y.; Chung, T.; Cao, C.; Kulprathipanja, S. The Effects of Polymer Chain Rigidification, Zeolite Pore Size and Pore Blockage on Polyethersulfone (PES)-Zeolite A Mixed Matrix Membranes. *J. Memb. Sci.* **2005**, *260*, 45–55. [CrossRef]
181. Erucar, I.; Yilmaz, G.; Keskin, S. Recent Advances in Metal–Organic Framework-Based Mixed Matrix Membranes. *Chem. Asian J.* **2013**, *8*, 1692–1704. [CrossRef] [PubMed]
182. Xin, Q.; Zhang, X.; Shao, W.; Li, H.; Zhang, Y. COF-Based MMMs with Light-Responsive Properties Generating Unexpected Surface Segregation for Efficient SO2/N2 Separation. *J. Memb. Sci.* **2023**, *665*, 121109. [CrossRef]
183. Zhang, Y.; Ma, L.; Lv, Y.; Tan, T. Facile Manufacture of COF-Based Mixed Matrix Membranes for Efficient $CO_2$ Separation. *Chem. Eng. J.* **2022**, *430*, 133001. [CrossRef]
184. Nasir, R.; Mukhtar, H.; Man, Z.; Mohshim, D.F. Material Advancements in Fabrication of Mixed-Matrix Membranes. *Chem. Eng. Technol.* **2013**, *36*, 717–727. [CrossRef]
185. Perez, E.; Karunaweera, C.; Musselman, I.; Balkus, K.; Ferraris, J. Origins and Evolution of Inorganic-Based and MOF-Based Mixed-Matrix Membranes for Gas Separations. *Processes* **2016**, *4*, 32. [CrossRef]
186. Goh, P.S.; Ismail, A.F.; Sanip, S.M.; Ng, B.C.; Aziz, M. Recent Advances of Inorganic Fillers in Mixed Matrix Membrane for Gas Separation. *Sep. Purif. Technol.* **2011**, *81*, 243–264. [CrossRef]
187. Ban, Y.; Li, Z.; Li, Y.; Peng, Y.; Jin, H.; Jiao, W.; Guo, A.; Wang, P.; Yang, Q.; Zhong, C.; et al. Confinement of Ionic Liquids in Nanocages: Tailoring the Molecular Sieving Properties of ZIF-8 for Membrane-Based $CO_2$ Capture. *Angew. Chem. Int. Ed.* **2015**, *54*, 15483–15487. [CrossRef] [PubMed]
188. Lin, R.; Ge, L.; Diao, H.; Rudolph, V.; Zhu, Z. Ionic Liquids as the MOFs/Polymer Interfacial Binder for Efficient Membrane Separation. *ACS Appl. Mater. Interfaces* **2016**, *8*, 32041–32049. [CrossRef] [PubMed]
189. Smith, S.J.D.; Lau, C.H.; Mardel, J.I.; Kitchin, M.; Konstas, K.; Ladewig, B.P.; Hill, M.R. Physical Aging in Glassy Mixed Matrix Membranes; Tuning Particle Interaction for Mechanically Robust Nanocomposite Films. *J. Mater. Chem. A Mater.* **2016**, *4*, 10627–10634. [CrossRef]
190. Mahdi, E.M.; Tan, J.-C. Dynamic Molecular Interactions between Polyurethane and ZIF-8 in a Polymer-MOF Nanocomposite: Microstructural, Thermo-Mechanical and Viscoelastic Effects. *Polymer* **2016**, *97*, 31–43. [CrossRef]
191. Shan, M.; Liu, X.; Wang, X.; Yarulina, I.; Seoane, B.; Kapteijn, F.; Gascon, J. Facile Manufacture of Porous Organic Framework Membranes for Precombustion $CO_2$ Capture. *Sci. Adv.* **2018**, *4*, aau1698. [CrossRef] [PubMed]
192. Gao, X.; Zou, X.; Ma, H.; Meng, S.; Zhu, G. Highly Selective and Permeable Porous Organic Framework Membrane for $CO_2$ Capture. *Adv. Mater.* **2014**, *26*, 3644–3648. [CrossRef] [PubMed]
193. Zhao, R.; Wu, H.; Yang, L.; Ren, Y.; Liu, Y.; Qu, Z.; Wu, Y.; Cao, L.; Chen, Z.; Jiang, Z. Modification of Covalent Organic Frameworks with Dual Functions Ionic Liquids for Membrane-Based Biogas Upgrading. *J. Memb. Sci.* **2020**, *600*, 117841. [CrossRef]
194. Liu, Y.; Wu, H.; Wu, S.; Song, S.; Guo, Z.; Ren, Y.; Zhao, R.; Yang, L.; Wu, Y.; Jiang, Z. Multifunctional Covalent Organic Framework (COF)-Based Mixed Matrix Membranes for Enhanced $CO_2$ Separation. *J. Memb. Sci.* **2021**, *618*, 118693. [CrossRef]
195. Keskin, S.; Alsoy Altinkaya, S. A Review on Computational Modeling Tools for MOF-Based Mixed Matrix Membranes. *Computation* **2019**, *7*, 36. [CrossRef]
196. Peters, L.; Hussain, A.; Follmann, M.; Melin, T.; Hägg, M.-B. $CO_2$ Removal from Natural Gas by Employing Amine Absorption and Membrane Technology—A Technical and Economical Analysis. *Chem. Eng. J.* **2011**, *172*, 952–960. [CrossRef]
197. Green, M.; Behbahani, H.S.; Yang, Y. Ammonium-Functionalized Polysulfone Copolymers for Moisture-Swing CO2 Capture 2023. U.S. Patent Application 17/793,925, 9 February 2023.
198. Green, M.; Korah, M.M.; Culp, K. Polymeric Materials for Carbon Dioxide Capture 2024. U.S. Patent Application 18/361,657, 1 February 2024.

199. IEA. Direct Air Capture. Available online: https://www.iea.org/energy-system/carbon-capture-utilisation-and-storage/direct-air-capture (accessed on 25 April 2024).
200. IEA. *CCUS around the World in 2021*; IEA: Paris, France, 2021; Available online: https://www.iea.org/reports/ccus-around-the-world-in-2021 (accessed on 1 April 2021).
201. Carbon Engineering Carbon Engineering Begins Work on Supporting Multi-Million Tonne Direct Air Capture Facilities in South Texas. Available online: https://carbonengineering.com/news-updates/multi-million-tonne-south-texas/ (accessed on 31 October 2022).
202. Baker Hughes Baker Hughes and HIF Global to Collaborate on Direct Air Capture Technology. Available online: https://investors.bakerhughes.com/node/27516/pdf (accessed on 7 March 2023).
203. CarbonCapture Project Bison. Available online: https://www.carboncapture.com/project-bison (accessed on 8 September 2022).
204. Energy Monitor Global Thermostat Unveils Direct Air Capture Plant in Colorado. Available online: https://www.energymonitor.ai/carbon-removal/global-thermostat-unveils-direct-air-capture-plant-in-colorado/?cf-view (accessed on 17 April 2023).
205. Carbon Engineering Engineering Begins on UK's First Large-Scale Facility That Captures Carbon Dioxide out of the Atmosphere. Available online: https://carbonengineering.com/news-updates/uks-first-large-scale-dac-facility/ (accessed on 23 June 2021).
206. Carbon Engineering New Partnership to Deploy Large-Scale Direct Air Capture in Norway. Available online: https://carbonengineering.com/news-updates/partnership-dac-norway/ (accessed on 23 November 2021).
207. Climeworks Capricorn. Available online: https://climeworks.com/plant-capricorn (accessed on 15 May 2017).
208. Climeworks Arctic Fox. Available online: https://climeworks.com/plant-arctic-fox (accessed on 15 October 2017).
209. Climeworks Orca: The First Large-Scale Plant. Available online: https://climeworks.com/plant-orca (accessed on 8 September 2021).
210. Climeworks Mammoth: Our Newest Facility. Available online: https://climeworks.com/plant-mammoth (accessed on 28 June 2022).
211. van der Giesen, C.; Kleijn, R.; Kramer, G.J. Energy and Climate Impacts of Producing Synthetic Hydrocarbon Fuels from $CO_2$. *Environ. Sci. Technol.* **2014**, *48*, 7111–7121. [CrossRef] [PubMed]
212. König, D.H.; Baucks, N.; Dietrich, R.-U.; Wörner, A. Simulation and Evaluation of a Process Concept for the Generation of Synthetic Fuel from $CO_2$ and $H_2$. *Energy* **2015**, *91*, 833–841. [CrossRef]
213. Ishaq, H.; Crawford, C. $CO_2$-based Alternative Fuel Production to Support Development of $CO_2$ Capture, Utilization and Storage. *Fuel* **2023**, *331*, 125684. [CrossRef]
214. Al-Sakkari, E.G.; Ragab, A.; Dagdougui, H.; Boffito, D.C.; Amazouz, M. Carbon Capture, Utilization and Sequestration Systems Design and Operation Optimization: Assessment and Perspectives of Artificial Intelligence Opportunities. *Sci. Total Environ.* **2024**, *917*, 170085. [CrossRef] [PubMed]
215. Yan, Y.; Borhani, T.N.; Subraveti, S.G.; Pai, K.N.; Prasad, V.; Rajendran, A.; Nkulikiyinka, P.; Asibor, J.O.; Zhang, Z.; Shao, D.; et al. Harnessing the Power of Machine Learning for Carbon Capture, Utilisation, and Storage (CCUS)—A State-of-the-Art Review. *Energy Environ. Sci.* **2021**, *14*, 6122–6157. [CrossRef]
216. Al-Sakkari, E.G.; Ragab, A.; So, T.M.Y.; Shokrollahi, M.; Dagdougui, H.; Navarri, P.; Elkamel, A.; Amazouz, M. Machine Learning-Assisted Selection of Adsorption-Based Carbon Dioxide Capture Materials. *J. Environ. Chem. Eng.* **2023**, *11*, 110732. [CrossRef]
217. Anderson, R.; Rodgers, J.; Argueta, E.; Biong, A.; Gómez-Gualdrón, D.A. Role of Pore Chemistry and Topology in the $CO_2$ Capture Capabilities of MOFs: From Molecular Simulation to Machine Learning. *Chem. Mater.* **2018**, *30*, 6325–6337. [CrossRef]